Electronic Supplementary Material (ESI) for New Journal of Chemistry.

Supporting Information

A Novel 3D Functional Cerium MOF with Lewis Base Sites and Lewis Acid Sites Used as Dual Functional Heterogeneous Catalysts for catalyzing Knoevenagel Condensation and Cyanosilylation

Peiran Zhao, Yuqian Liu, Cheng He, and Chunying Duan*

State Key Laboratory of Fine Chemicals, Dalian University of Technology, Dalian 116024, China

Table S1. Crystal data and structure refinements for Ce-4L and Tb-4L.

	Ce-4L	Tb-4L
Empirical formula	$C_{16}H_{15}O_{12}NCe$	$C_{16}H_{15}O_{12}NTb$
Formula weight	553.413	572.222
Wavelength (Å)	0.71073	0.71073
Crystal size (mm)	0.24×0.24×0.22	0.24×0.22×0.20
Temperature (K)	210 (2)	296
Crystal system	Orthorhombic	Orthorhombic
Space group	*P*nna	*P*nna
a (Å)	8.9711(17)	8.9732(6)
b (Å)	13.667(3)	13.3957(8)
c (Å)	14.756(3)	14.6655(9)
Volume ($Å^3$)	1809.2(6)	1762.83(19)
Z	4	4
Calculated density (Mg/m^3)	2.032	2.156
Absorption coefficient **(mm^{-1})**	2.588	4.085
F **(000)**	1088.689	1117.031
ϑ **range for data collection (deg)**	3.05-27.45	3.90-24.99
Limiting indices	-11<=h<=11	-11<=h<=11
	-11<=k<=17	-16<=k<=17
	-19<=l<=19	-19<=l<=18
Reflections collected / unique	13550 / 1588	15940 / 1537
	[R_{int} = 0.0263]	[R_{int} = 0.0689]
Completeness to **θ = 25.00**	0.9931	0.9853
Data / restraints / parameters	1588 / 0 / 124	1537 / 0 / 124
Goodness-of-fit on F^2	1.0642	1.0523
Final **R** indices [I>2σ(I)]	R_1 = 0.0252;	R_1 = 0.0358;
	wR_2 = 0.0666	wR_2 = 0.0733
R **indices (all data)**	R_1 = 0.0282;	R_1 = 0.0503;
	wR_2 = 0.0697	wR_2 = 0.0799
Largest diff. Peak and hole($e·Å^{-3}$)	1.0588 and -0.5725	1.2613 and -1.2759
CCDC No.	2265265	2265266.

$^a R_1 = \sum||F_o| - |F_c||/\sum|F_o|$; $^b wR_2 = [\sum w(|F_o|^2 - |F_c|^2)^2/\sum w(F_o^2)^2]^{1/2}$; $w = 1/[\sigma^2(F_o^2) + (aP)^2 + bP]$, $P = (F_o^2 + 2F_c^2)/3$.

Table S2. Selected Bond lengths [Å] and angles [deg] for Ce-4L.

Ce-4L			
Ce(1)-O(1)	2.403(4)	Ce(1)-O(2)#1	2.473(3)
Ce(1)-O(2)#2	2.473(3)	Ce(1)-O(3)#3	2.583(3)
Ce(1)-O(3)#4	2.583(3)	Ce(1)-O(4)#4	2.642(3)
Ce(1)-O(4)#3	2.642(3)	O(2)#2-Ce(1)-O(1)	76.83(11)
O(2)#2-Ce(1)-O(1)	96.14(10)	O(2)#1-Ce(1)-O(1)	96.14(10)
O(2)#1-Ce(1)-O(1)	76.83(11)	O(2)#1-Ce(1)-O(2)#2	155.85(14)
O(3)#4-Ce(1)-O(1)	74.77(9)	O(3)#4-Ce(1)-O(1)	136.20(10)
O(3)#3-Ce(1)-O(1)	136.20(10)	O(3)#3-Ce(1)-O(1)	74.77(9)
O(3)#3-Ce(1)-O(2)#2	124.40(10)	O(3)#4-Ce(1)-O(2)#1	124.40(10)
O(3)#4-Ce(1)-O(2)#2	76.57(9)	O(3)#3-Ce(1)-O(2)#1	76.57(9)
O(3)#3-Ce(1)-O(3)#4	74.60(12)	O(4)#4-Ce(1)-O(1)	138.07(9)
O(4)#4-Ce(1)-O(1)	67.55(10)	O(4)#4-Ce(1)-O(1)	138.07(9)
O(4)#3-Ce(1)-O(1)	67.55(130)	O(4)#3-Ce(1)-O(2)#2	75.07(9)
O(4)#4-Ce(1)-O(2)#1	75.07(9)	O(4)#3-Ce(1)-O(2)#1	121.33(8)
O(4)#4-Ce(1)-O(2)#2	121.33(8)	O(4)#4-Ce(1)-O(3)#4	50.42(8)
O(4)#3-Ce(1)-O(3)#4	68.87(9)	O(4)#4-Ce(1)-O(3)#3	68.87(9)
O(4)#3-Ce(1)-O(3)#3	50.42(8)	O(4)#3-Ce(1)-O(4)#4	102.33(13)

Symmetry transformations used to generate equivalent atoms:

#1: -x, -y, -z+1; #2: x+1/2, y, -z+1; #3: x, -y-1/2, -z+3/2; #4: -x+1/2, y-1/2, -z+3/2.

Crystallograph:

For Ce-H4L

A colourless block-shaped-shaped crystal with dimensions 0.24 × 0.24 × 0.22 mm^3 was mounted. Data were collected using a Bruker APEX-II CCD diffractometer operating at T = 210(2) K.

Data were measured using ϕ and ω scans with Mo Kα radiation. The diffraction pattern was indexed and the total number of runs and images was based on the strategy calculation from the program BrukerAPEX2. The maximum resolution that was achieved was Θ = 25.00° (0.84 Å).

The unit cell was refined using Bruker SAINT on 6070 reflections, 45% of the observed reflections.

Data reduction, scaling and absorption corrections were performed using Bruker SAINT. The final completeness is 99.31 % out to 25.00° in Θ. SADABS 2016/2 was used for absorption correction. R(int)was 0.0245 after correction. The Ratio of minimum to maximum transmission is 0.4913 and 0.5629.

The absorption coefficient μ of this material is 2.588 mm^{-1} at this wavelength (λ = 0.71073Å) and the minimum and maximum transmissions are 0.491 and 0.563.

The structure was solved and the space group *Pnna* (# 52) determined by the ShelXT 2014/5 (Sheldrick, 2014) structure solution program using using iterative methods and refined by full matrix least squares minimisation on $\boldsymbol{F^2}$ using version of olex2. refine 1.5-alpha (Bourhis et al., 2015). All non-hydrogenatoms were refined anisotropically. Hydrogen atom positions were calculated geometrically and refined using the riding model. Hydrogen atom positions were calculated geometrically and refined using the riding model.

_exptl_absorpt_process_details: SADABS 2016/2 was used for absorption correction. R(int) was 0.0245
after correction. The Ratio of minimum to maximum transmission is 0.4913 and 0.5629

_smtbx_masks_special_details: A solvent mask was calculated and 108 electrons were found in a volume of 344$Å^3$ in 1 void per unit cell. This is consistent with the presence of 3[H2O] per Formula Unit which account for 120 electrons per unit cell.

For Tb-H4L:

A colourless block-shaped-shaped crystal with dimensions 0.24 × 0.22 × 0.20 mm^3 was mounted. Data were collected using a Bruker APEX-II CCD diffractometer operating at T = 296(2) K.
Data were measured using ϕ and ω scans with Mo Kα radiation. The diffraction pattern was indexed and the total number of runs and images was based on the strategy calculation from the program Bruker APEX2. The maximum resolution that was achieved was Θ = 24.99° (0.84 Å). The unit cell was refined using Bruker SAINT on 5736 reflections, 36% of the observed reflections.
Data reduction, scaling and absorption corrections were performed using Bruker SAINT. The final completeness is 98.53 % out to 24.99° in Θ. SADABS. The absorption coefficient μ of this material is 4.085 mm^{-1} at this wavelength (λ = 0.71073Å) and the minimum and maximum transmissions are 0.259 and 0.333.
The structure was solved and the space group *Pnna* (# 52) determined by the ShelXT 2018/2 (Sheldrick, 2018) structure solution program using using dual methods and refined by full matrix least squares minimisation on $\boldsymbol{F^2}$ using version of olex2.refine 1.5-alpha (Bourhis et al., 2015). All non-hydrogen atoms were refined anisotropically. Hydrogen atom positions were calculated geometrically and refined using the riding model. Hydrogen atom positions were calculated geometrically and refined using the riding model.

_exptl_absorpt_special_details: SADABS 2016/2 was used for absorption correction. R(int) was 0.0355 after correction. The Ratio of minimum to maximum transmission is 0.2587 and 0.3334.

_exptl_absorpt_process_details: SADABS *_smtbx_masks_special_details*: A solvent mask was calculated and 120 electrons were found in a volume of 348$Å^3$ in 1 void per unit cell. This is consistent with the presence of 3[H2O] per Formula Unit which account for 120 electrons per unit cell.

Citations

APEX2 suite for crystallographic software, Bruker axs, Madison, WI (2019).

L.J. Bourhis and O.V. Dolomanov and R.J. Gildea and J.A.K. Howard and H. Puschmann, The Anatomy of a Comprehensive Constrained, Restrained, Refinement Program for the Modern Computing Environment Olex2 Disected, *Acta Cryst. A*, (2015), **A71**, 59-71.

O.V. Dolomanov and L.J. Bourhis and R.J. Gildea and J.A.K. Howard and H. Puschmann, Olex2: A complete structure solution, refinement and analysis program, *J. Appl. Cryst.*, (2009), **42**, 339-341.

SAINT - Software for the Integration of CCD Detector System Bruker Analytical X-ray Systems, Bruker axs, Madison, WI (2019).

Sheldrick, G.M., ShelXT-Integrated space-group and crystal-structure determination, *Acta Cryst.*, (2015), **A71**, 3-8.

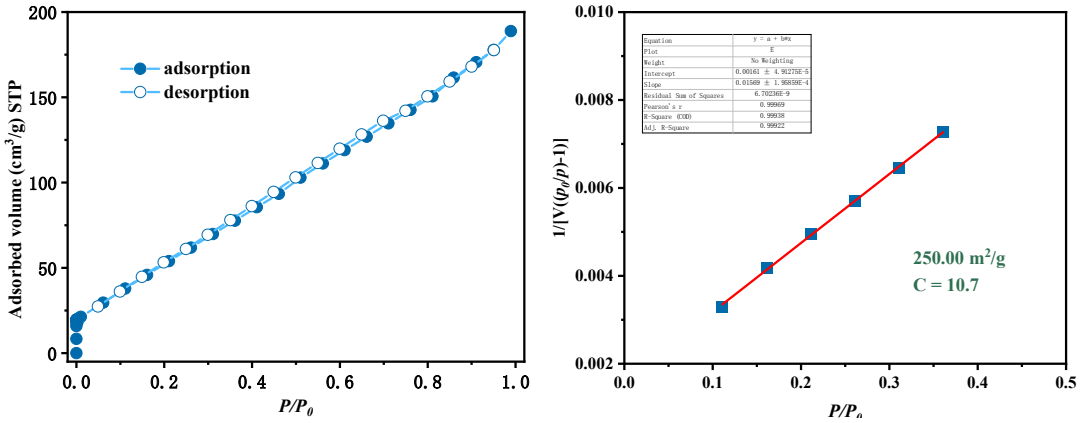

Figure S1. N_2 adsorption isotherm of activated Ce-4L.

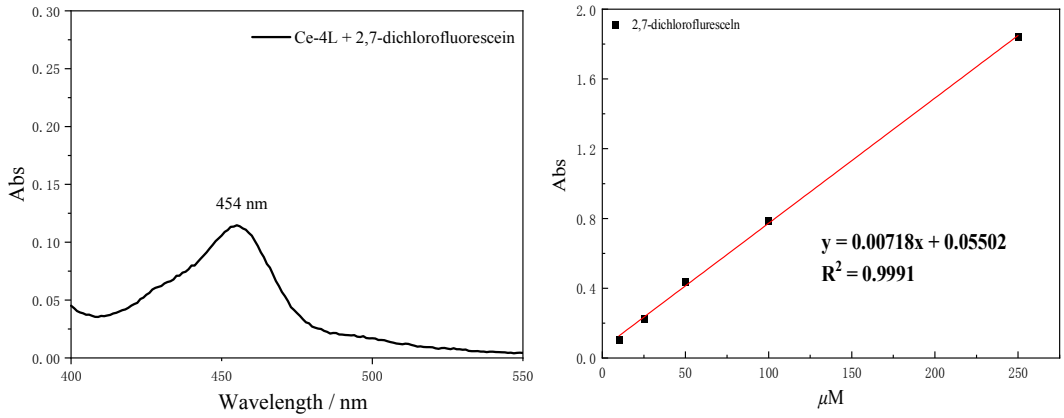

Figure S2. (a) The UV-Vis absorption spectra of 2',7'-dichlorofluorescein; (b) The corresponding standard curve.

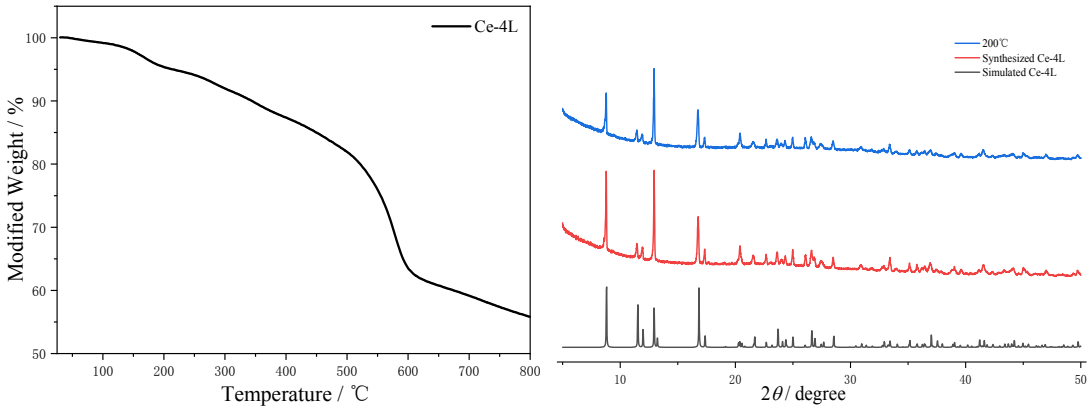

Figure S3. (a) TGA plot of Ce-4L; (b) PXRD of Ce-4L.

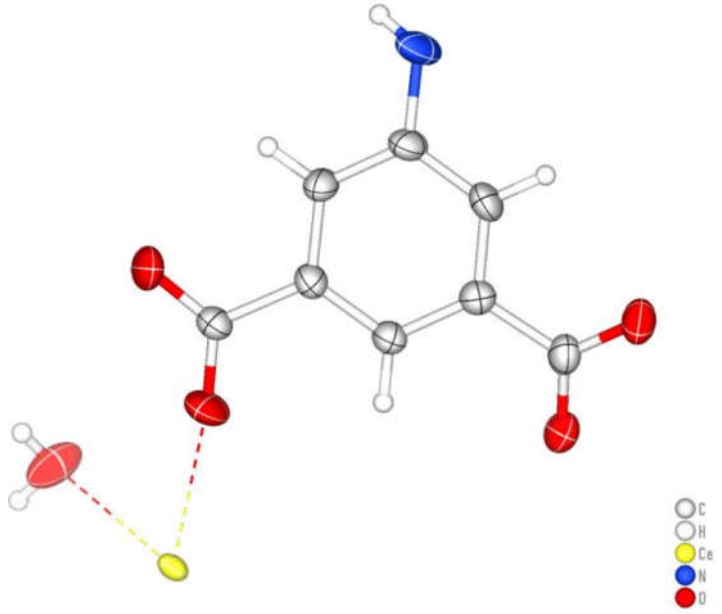

Figure S4. (a) The metal ion and ligand in asymmetric unit of Ce-4L.

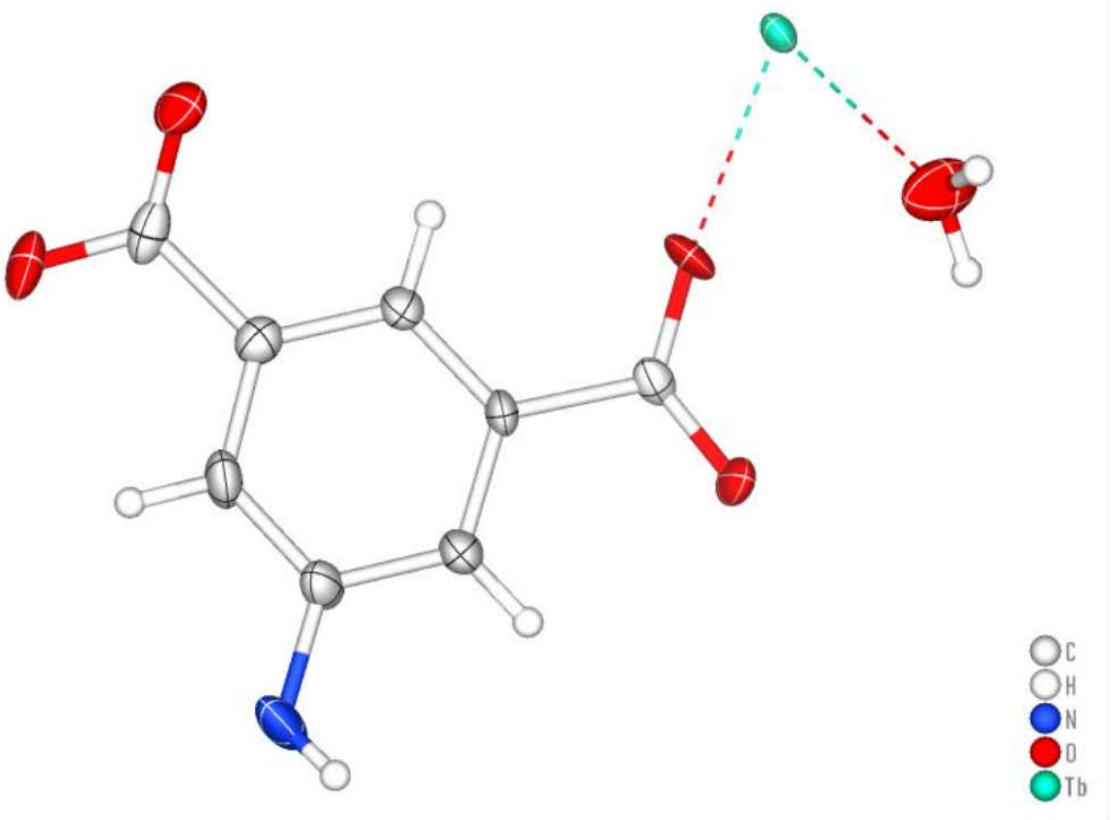

Figure S4. (b) The metal ion and ligand in asymmetric unit of Tb-4L.

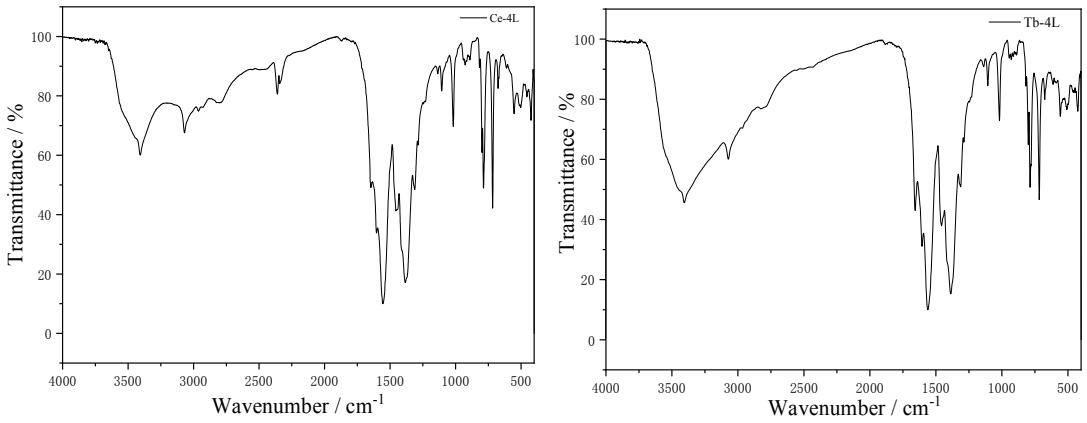

Figure S5. (a) FT-IR spectrum of Ce-4L; (b) FT-IR spectrum of Tb-4L.

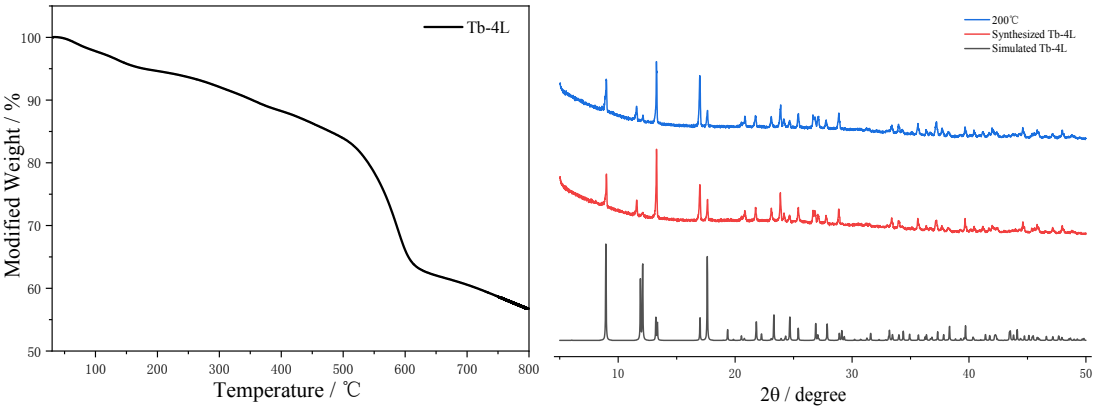

Figure S6. (a) TGA plot of Tb-4L; (b) PXRD of Tb-4L.

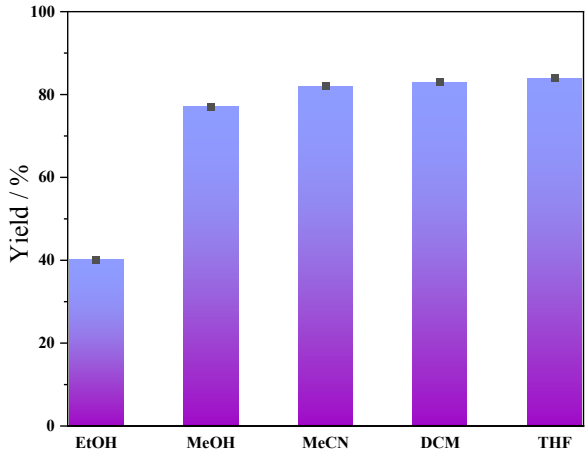

Figure S7. The cyanosilylation yields in different solutions with 0.01 mmol Ce-4L (0.5 mmol 3-methoxybenzaldehyde, 1.2 mmol TMSCN, in 2 mL solution, under Ar condition).

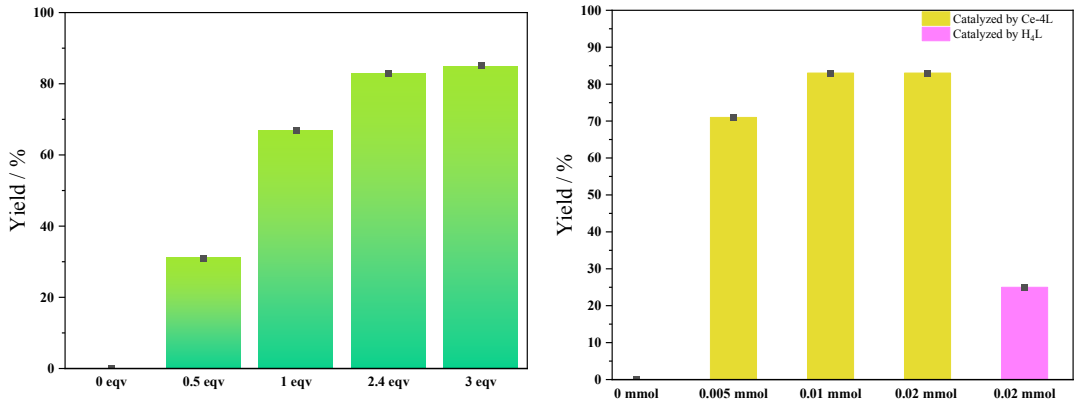

Figure S8. (a) The yields for cyanosilylation with different amounts of TMSCN (0.5 mmol 3-methoxybenzaldehyde, 0.01 mmol Ce-4L, in 2 mL DCM at room temperature); (b) The yields for cyanosilylation with different amounts of Ce-4L (0.5 mmol 3-methoxybenzaldehyde, 1.2 mmol TMSCN, in 2 mL DCM at room temperature).

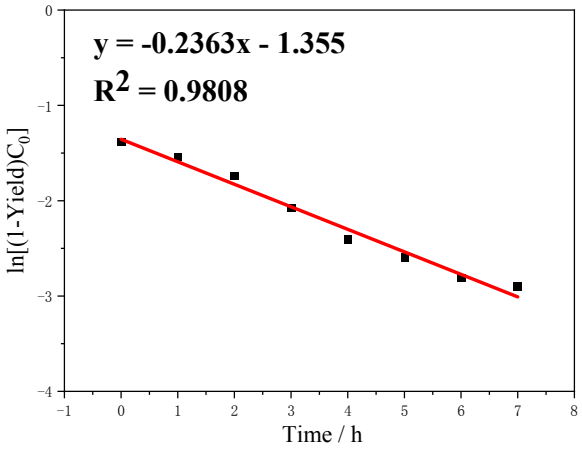

Figure S9. One-order reaction dynamics equation for cyanosilylation catalysed by Ce-4L.

Table S3. Comparison of other MOFs used as catalysts for catalysing Knoenenagel condensation.

Entry	Catalyst	Substrate	Solvent	Temp. (℃)	Time (h)	Yield (%)	Ref.
1	Pr-DSB	Benzaldehyde	Solvent-free	50	3	78	37
2	Yb-MOF	Benzaldehyde	Solvent-free	r.t.	12	84	56
3	Ce-MOF	Benzaldehyde	Solvent-free	r.t.	2	94	57
4	Nd(btc)	Benzaldehyde	DCM	r.t.	2	88	58
5	UiO-66	Benzaldehyde	Solvent-free	r.t.	3	68	59
6	MIL-101	Benzaldehyde	Heptane	r.t.	4	87	59
7	MOF-74	4-Methoxybenzaldehyde	Solvent-free	60	0.5	58	60
8	Zn-STU-2	4-Biphenyladehyde	DCM	100	12	70	61
9	Tb-TCA	2-Nitrobenzaldehyde	DCM	r.t.	4	78	62
10	Ce-4L	3-Methoxybenzaldehyde	DCM	r.t.	12	83	This work

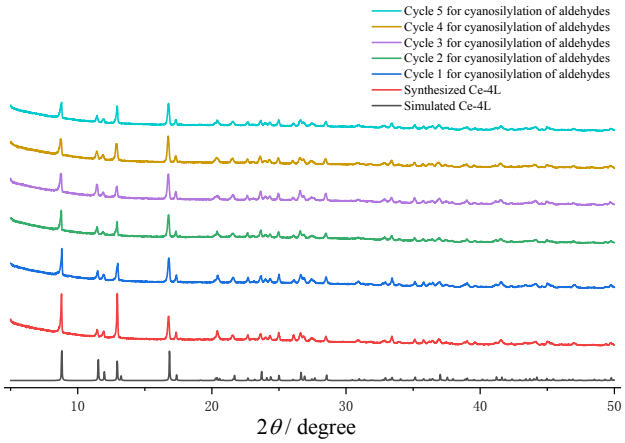

Figure S10. PXRD of Ce-4L after 5 cycles for catalyzing cyanosilylation.

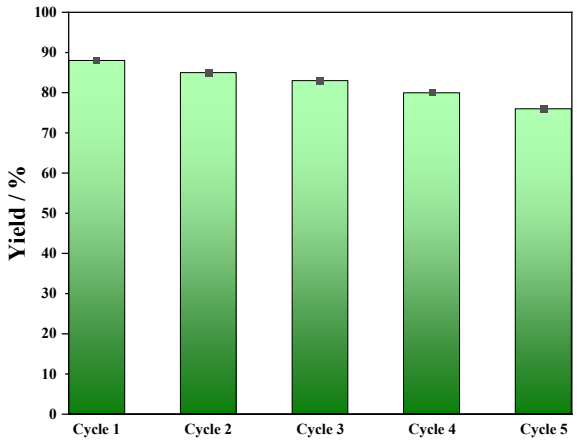

Figure S11. The cyanosilylation yields for 5 cycles (0.5 mmol 3-methoxybenzaldehyde, 1.2 mmol TMSCN, 0.01 mmol Tb-4L, in 2 mL DCM at room temperature under Ar condition).

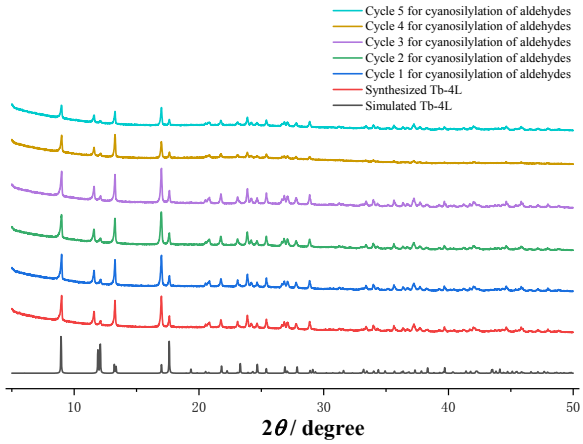

Figure S12. PXRD of Tb-4L after 5 cycles for catalyzing cyanosilylation.

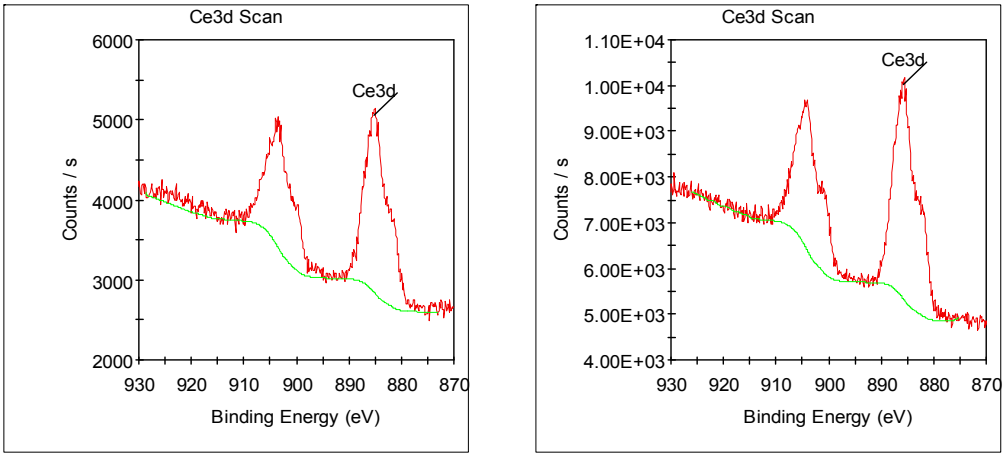

Figure S13. XPS spectra of Ce-4L and Ce-4L treated with 3-nitrobenzaldehyde. (a) Ce 3d of Ce-4L; (b) Ce 3d of Ce-4L treated with 3-nitrobenzaldehyde.

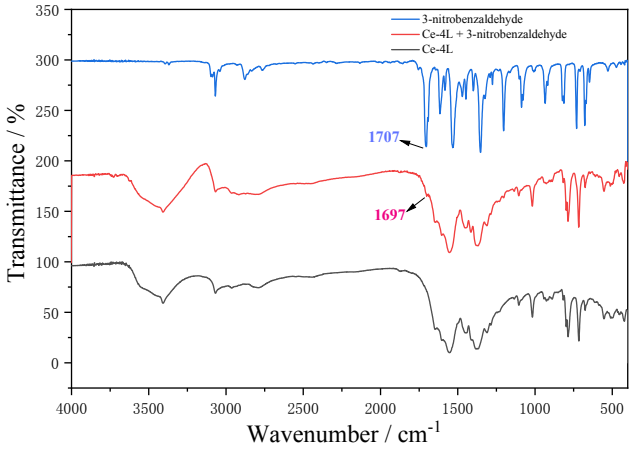

Figure S14. FT-IR spectrum of Ce-4L immersed in 3-nitrobenzaldehyde.

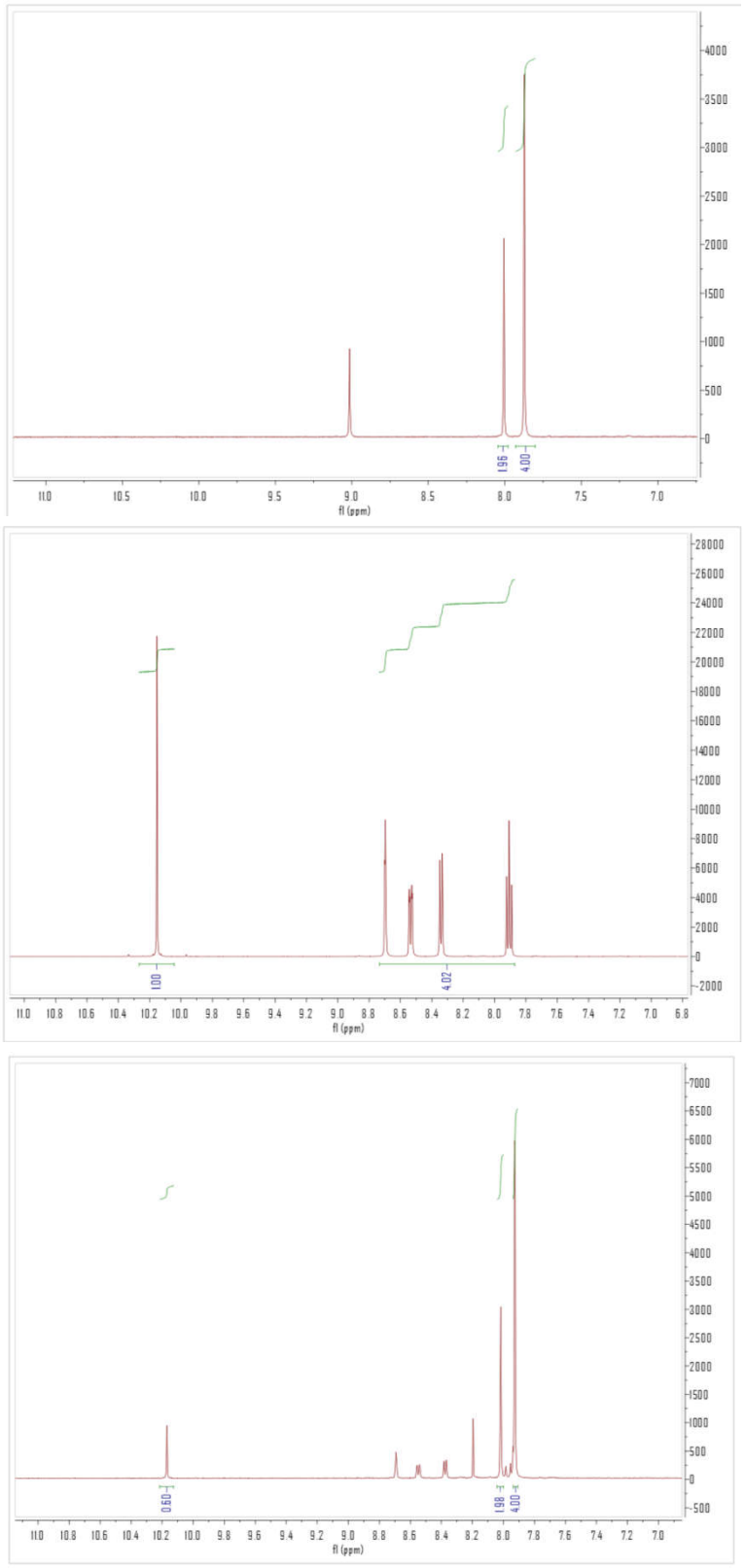

Figure S15. (a) ^{1}H-NMR spectrum of H_4L; (b) ^{1}H-NMR spectrum of 3-nitrobenzaldehyde; (c) ^{1}H-NMR spectrum of Ce-4L immersed in 3-nitrobenzaldehyde then treated with DCl.

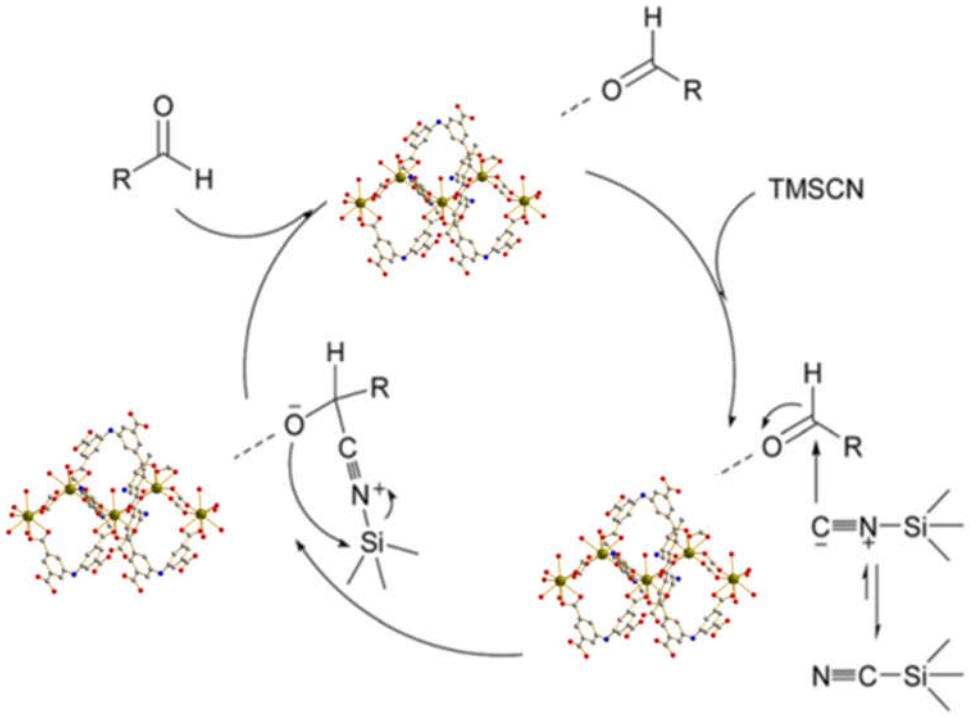

Figure S16. The possible mechanism of cyanosilylation catalyzed by Ce-4L.

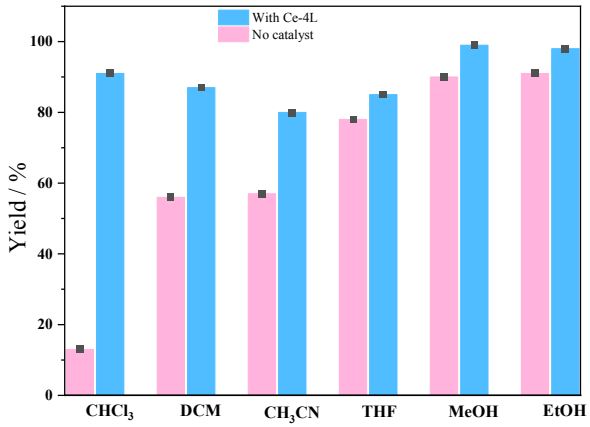

Figure S17. The Knoenenagel condensation yields in different solutions with 0.01 mmol Ce-4L (0.5 mmol 3-methoxybenzaldehyde, 1.2 mmol malononitrile, in 2 mL solution).

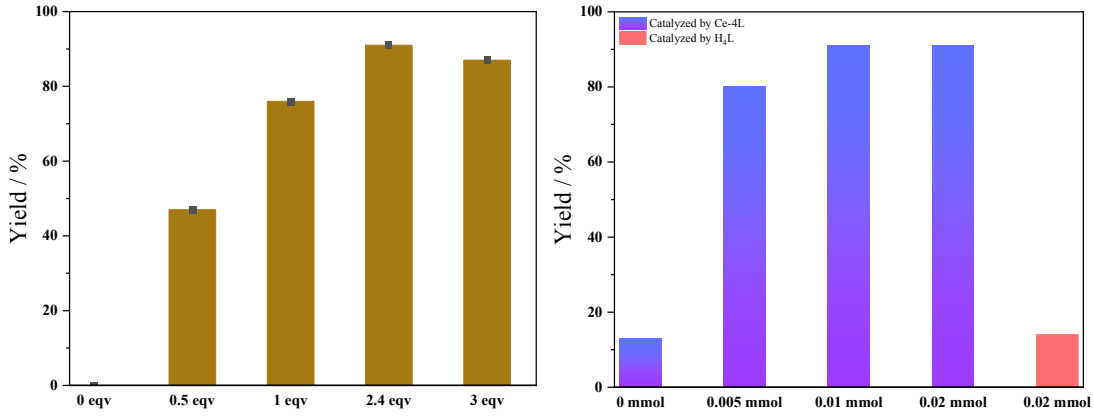

Figure S18. (a) The yields for Knoevenagel condensation with different amounts of malononitrile (0.5 mmol 3-methoxybenzaldehyde, 0.01 mmol Ce-4L, in 2 mL chloroform at room temperature); (b) The yields for Knoevenagel condensation with different amounts of Ce-4L (0.5 mmol 3-methoxybenzaldehyde, 1.2 mmol malononitrile, in 2 mL chloroform at room temperature).

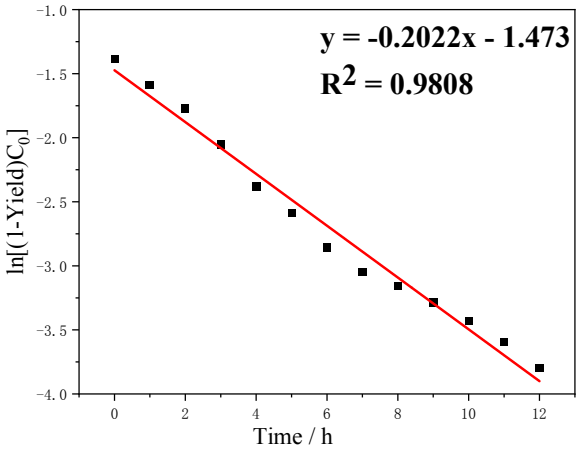

Figure S19. One-order reaction dynamics equation for Knoenenagel condensation catalysed by Ce-4L.

Table S4. Comparison of other MOFs used as catalysts for catalysing Knoenenagel condensation.

Entry	Catalyst	Substrate	Solvent	Temp. (℃)	Time (h)	Yield (%)	Ref.
1	Zn-MOF-NH_2	Benzaldehyde	DMF	80	4.5	98	73
2	CAU-1-NH_2	Benzaldehyde	Ethanol	40	7	98	74
3	ZIF-8	Benzaldehyde	Toluene	r.t.	6	97	75
4	ZIF-9	Benzaldehyde	Toluene	r.t.	6	99	76
5	TMU-5	Benzaldehyde	Methanol	r.t.	0.5	68	77
6	UPC-30	Benzaldehyde	DCM	r.t.	5	94	78
7	NUC-58a	4-Nitrobenzaldehyde	Ethanol	65	7	98	79
8	Tb-DCBA	4-Nitrobenzaldehyde	DCM	r.t.	6	67	80
9	ZnMOF	4-Methoxybenzaldehyde	Methanol	r.t.	2	70	81
10	Ce-4L	3-Methoxybenzaldehyde	Chloroform	r.t.	12	91	This work

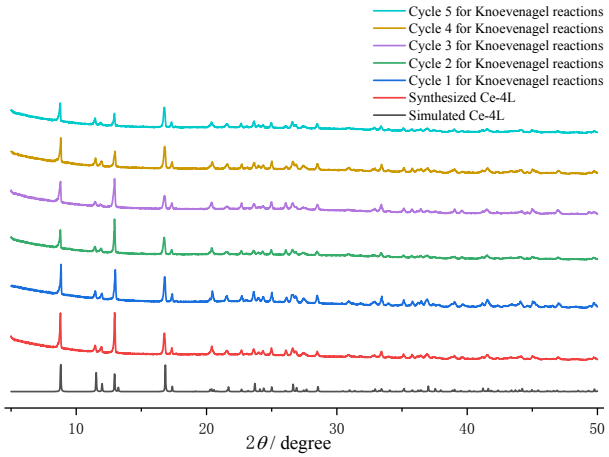

Figure S20. PXRD of Ce-4L after 5 cycles for catalyzing Knoevenagel condensation.

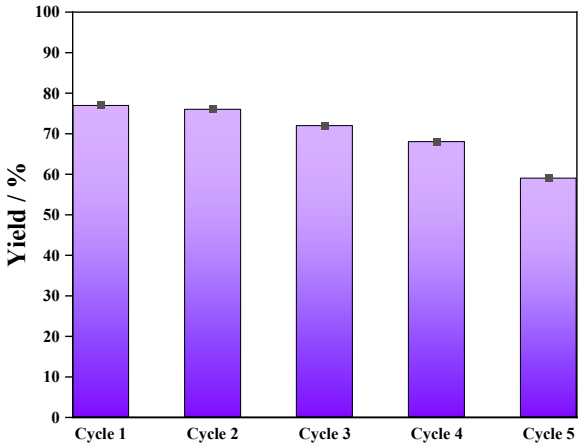

Figure S21. The Knoenenagel condensation yields for 5 cycles (0.5 mmol 3-methoxybenzaldehyde, 1.2 mmol malononitrile, 0.01 mmol Tb-4L, in 2 mL chloroform at room temperature).

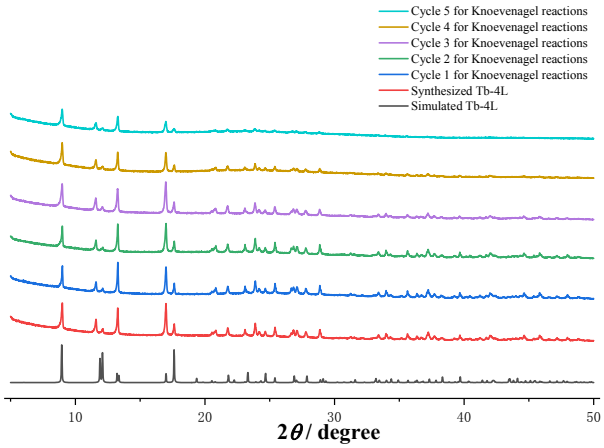

Figure S22. PXRD of Tb-4L after 5 cycles for catalyzing Knoevenagel condensation.

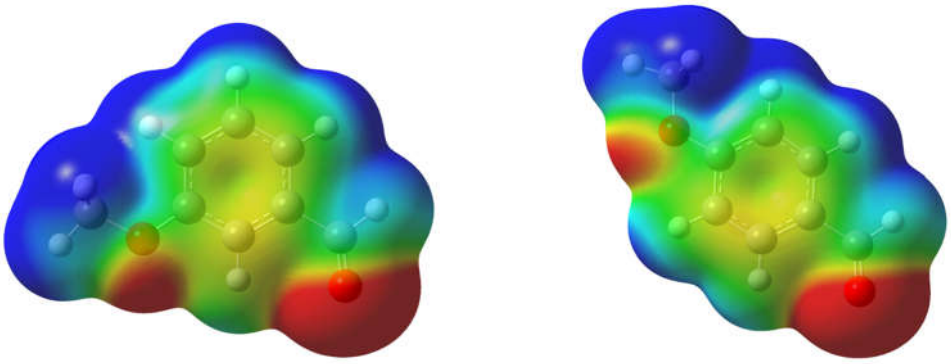

Figure S23. (a) The electron distribution of 3-methoxybenzaldehyde; (b) The electron distribution of 4-methoxybenzaldehyde.

^{1}H-NMR Data

^{1}H-NMR Spectral Data of H_4L.

(400 MHz, DMSO) δ 7.54(4 H), 8.01(2H), 9.09 (H), 13.23 (4H) ppm.[1]

^{1}H-NMR Spectral Data of TMSCN.

(500 MHz, $CDCl_3$) δ 0.30 (9H, s, $SiCH_3$).

^{1}H-NMR Spectral Data of 1,3,5-Trimethoxybenzene.

(500 MHz, $CDCl_3$) δ 3.78 (9H, s, OCH_3), 6.10 (3H, s, ArH).[2]

^{1}H-NMR Spectral Data of Different Aldehydes.

2-Nitobenzaldehyde (400 MHz, $CDCl_3$): δ 10.40 (s, 1H, CHO), 8.10 (dd, *J* = 7.6, 1.6 Hz, 1H, Ar-CH), 7.90 (dd, *J* = 7.2, 1.6 Hz, 1H, Ar-CH), 7.80-7.70 (m, 2H, Ar-CH).[3]

3-Nitobenzaldehyde (400 MHz, $CDCl_3$) δ 10.12 (s, 1H), 8.71 (dd, *J* = 2.3, 1.6 Hz, 1H), 8.50-8.47 (m, 1H), 8.25-8.22 (m, 1H), 7.79-7.75 (m, 1H).[4]

4-Nitobenzaldehyde (400 MHz, $CDCl_3$): δ 10.18 (s, 1H, CHO), 8.41 (d, *J* = 8.0 Hz, 2H, Ar-CH), 8.10 (d, *J* = 8.0 Hz, 2 H, Ar-CH).[3]

2-Naphthaldehyde (400 MHz, $CDCl_3$) δ 10.37 (s, 1H), 9.26 (d, *J* = 8.7 Hz, 1H), 8.06 (d, *J* = 8.2 Hz, 1H), 7.94 (dd, *J* = 7.1, 1.2 Hz, 1H), 7.89 (d, *J* = 8.2 Hz, 1H), 7.70-7.65 (m, 1H), 7.61-7.55 (m, 2H).[5]

***o*-Methoxybenzaldehyde** (500 MHz, $CDCl_3$) δ 10.45 (s, 1H), 7.82-7.80 (dd, 1H, *J* = 9.6, 2.3 Hz), 7.56-7.51 (ddd, 1H, *J* = 10.6, 9.2, 2.3 Hz), 7.03-6.96 (m, 2H), 3.91 (s, 3H).[6]

***m*-Methoxybenzaldehyde** (400 MHz, $CDCl_3$) δ 9.94 (s, 1H), 7.45-7.38 (m, 2H), 7.36 (d, *J* = 1.9 Hz, 1H), 7.16-7.13 (m, 1H), 3.83 (s, 3H).[5]

***p*-Methoxybenzaldehyde** (400 MHz, $CDCl_3$): δ 9.83 (s, 1H, CHO), 8.17-7.55 (m, 2H, Ar-CH), 6.59 (d, *J* = 8.7Hz, 2H, Ar-CH), 3.83 (m, 3H, OCH_3).[3]

Heptanal (400 MHz, $CDCl_3$) δ 9.74 (s, 1H), 2.38 (t, 2H), 1.63-1.57 (m, 2H), 1.39-1.21 (m, 6H), 0.90-0.83 (t, 3H).[7]

Salicylaldehyde (500 MHz, $CDCl_3$) δ 11.06 (s, 1H, -OH), 9.93 (s, 1H, -CHO), 7.60 (m, 1H, ArH), 7.56 (m, 1H, ArH), 7.07 (m, 1H, ArH), 7.03 (m, 1H, ArH).[8]

4-Biphenylcarboxaldehyde (500 MHz, $CDCl_3$) δ 7.40-7.52 (3H, m, H-Ar), 7.75 (2H, d, *J* = 7.6 Hz, H-Ar), 7.86 (2H, d, *J* = 6.8 Hz, H-Ar), 7.98 (2H, d, *J* = 6.8 Hz, H-Ar), 10.05 (1H, s, CHO).[9]

4-(Diethylamino)salicylaldehyde (400 MHz, $CDCl_3$) δ 11.65 (br, 1H), 9.49 (s, 1H), 7.27 (d, *J* = 8.8 Hz, 1H), 6.27 (d, *J* = 10.2 Hz, 1H), 6.08 (s, 1H), 3.41 (q, *J* = 7.0 Hz, 4H), 1.22 (t, *J* = 7.1 Hz, 6H).[10]

4-Benzyloxybenzaldehyde (400 MHz, $CDCl_3$) δ 5.15 (2H, s, $PhCH_2$), 7.08 (2H, d, *J* = 8.7 Hz, ArH), 7.34-7.47 (5H, m, ArH overlapping), 7.84 (2H, d, *J* = 8.8 Hz, ArH) and 9.89 (1H, s, HC=O).[11]

Benzaldehyde (400 MHz, $CDCl_3$) δ 9.94 (s, 1H), 7.81 (d, J = 6.8 Hz, 2H), 7.55 (t, J = 7.4 Hz, 1H), 7.45 (t, J = 7.5 Hz, 2H).[12]

***p*-Chlorobenzaldehyde** (250 MHz, $CDCl_3$) δ 9.96 (s, 1H, CHO), 7.80 (d, J = 8.2 Hz, 2H, 2 CH), 7.49 (d, *J* = 8.2 Hz, 2H, 2CH).[13]

^{1}H-NMR Spectral Data of the Product of Different Aldehydes in Cyanosilylation

The product of 2-Nitobenzaldehyde ^{1}H-NMR (500 MHz, $CDCl_3$): δ 8.18-8.20 (d, 1H, *J* = 8.20 Hz), 7.97-7.99 (d, 1H, *J* = 8.20 Hz), 7.78-7.82 (t, 1H, *J* = 7.80 Hz), 7.63-7.66 (t, 1H, *J* = 7.80 Hz), 6.20 (s, 1H), 0.07 (s, 9H).[14]

The product of 3-Nitobenzaldehyde (300 MHz, $CDCl_3$): δ 0.29 (s, 9H, $Si(CH_3)_3$), 5.60 (s, 1H, $CHOSi(CH_3)_3$), 7.63 (t, *J* = 4.5 Hz, 1H, Ph), 7.84 (d, J = 6.0 Hz, 1H, Ph), 8.26 (d, J = 8.0 Hz, 1H, Ph) , 8.34 (s,1H, Ph).[15]

The product of 4-Nitobenzaldehyde (600 MHz, $CDCl_3$): δ 0.29 (s, 9 H, $Si(CH_3)_3$), 5.64 (s, 1 H, OCHCN), 6.68 (d, *J* = 8.4 Hz, 2 H, ArH), 8.28 (d, *J* = 8.4 Hz, 2 H, ArH).[16]

The product of 2-Naphthaldehyde (200 MHz, $CDCl_3$): δ 0.11 (s, 9H, $Si(CH_3)_3$, 5.95 (s, 1H, $CHOSi(CH_3)_3$), 7.37-7.63(m, 4H, Ph), 7.78(d, *J* = 7.5 Hz, 2H, Ph), 8.07(d, *J* = 8.0 Hz, 1H, Ph).[17]

The product of *o*-Methoxybenzaldehyde (300 MHz, $CDCl_3$) δ 7.62-7.58 (m, 1 H), 7.40-7.33 (m, 1 H), 7.08-6.98 (m, 1 H), 6.94-6.86 (m, 1 H), 5.81 (s, 1 H), 3.89 (s, 3 H), 0.41-0.14 (m, 9 H).[18]

The product of *m*-Methoxybenzaldehyde (400 MHz, $CDCl_3$) δ 7.32 (t, 1H, J = 7.9 Hz, aromatics), 7.05-7.02 (m, 2H, aromatics), 6.92 (dd, 1H, J = 8.2, 2.0 Hz aromatic), 5.47 (s, 1H, CHCN), 3.83 (s, 3H, CH_3O), 0.24 (s, 9H, $Si(CH_3)_3$).[19]

The product of *p*-Methoxybenzaldehyde (250 MHz, $CDCl_3$): δ 7.38 (d, 2H, *J* = 8.8 Hz, Ph-2H, 6H), 6.92 (d, 2H, *J* = 8.8 Hz, Ph-3H, 5H), 5.43 (s, 1H, CH), 3.82 (s, 3H, OCH_3), 0.21 (s, 9H, $(CH_3)_3$).[20]

The product of Salicylaldehyde δ 11.50 (br, 1H), 7.62-7.58 (m, 1H), 7.40-7.33 (m, 1H), 7.08-6.98 (m, 1H), 6.94-6.86 (m, 1H), 5.57 (s, 1H), 0.22(s, 9H).[21]

The product of 4-Biphenylcarboxaldehyde (400 MHz, $CDCl_3$): δ 7.60−7.51 (m, 7H), 7.45−7.41 (m, 2H), 7.36−7.33 (m, 1H), 5.53 (s, 1H), 0.25 (s, 9H).[22]

The product of 4-(Diethylamino)salicylaldehyde (400 MHz, $CDCl_3$) δ 11.50 (br, 1H), 7.27 (d, *J* = 8.8 Hz, 1H), 6.27 (d, *J* = 10.2 Hz, 1H), 6.08 (s, 1H), 3.41 (q, *J* = 7.0 Hz, 4H), 1.22 (t, *J* = 7.1 Hz, 6H), 0.25 (s, 9H).[23]

The product of 4-Benzyloxybenzaldehyde (200 MHz, $CDCl_3$) δ 0.22 (s, 9H), 5.46 (s, 1H), 6.99-7.13 (m, 5H), 7.31-7.44 (m, 4H).[24]

The product of Benzaldehyde (400 MHz, $CDCl_3$) δ 7.43-7.28 (m, 5H), 5.42 (s, 1H), 0.16 (s, 9H).[25]

^{1}H-NMR Spectral Data of the Product of Different Aldehydes in Knoevenagel Condensation

The product of Benzaldehyde (500 MHz, $CDCl_3$) δ 7.92 (2 H, d, *J* =7.63 Hz), 7.79 (1H, s), 7.64 (1 H, d, *J* =7.25 Hz), 7.53-7.58 (2H, m).[26]

The product of 2-Nitobenzaldehyde (400 MHz, $CDCl_3$) δ 8.45 (s, 1H), 8.36 (d, *J* = 8.4 Hz, 1H), 7.91-7.79 (m, 3H).[27]

The product of 3-Nitobenzaldehyde (300 MHz, $CDCl_3$) δ 8.64 (s, 1H), 8.35 (d, *J* = 8.2 Hz, 1H), 8.21 (d, *J* = 7.9 Hz, 1H), 8.02 (s, 1H), 7.68 (t, *J* = 8.1 Hz, 1H).[28]

The product of 4-Nitobenzaldehyde (400 MHz, DMSO) δ 8.73 (1H, s), 8.42 (2H, dd, *J* = 17.3, 10.4), 8.25-8.06 (2 H, m), 3.45 (1H, s), 2.51 (1H, s).[29]

The product of 2-Naphthaldehyde (600 MHz, DMSO-d_6) δ 8.68 (s, 1H), 8.51-8.47 (m, 1H), 8.14 (d, *J* = 8.7 Hz, 1H), 8.11-8.06 (m, 2H), 8.04 (dd, *J* = 8.2, 1.1 Hz, 1H), 7.75 (ddd, *J* = 8.2, 6.8, 1.3 Hz, 1H), 7.68 (ddd, *J* = 8.1, 6.8, 1.2 Hz, 1H).[30]

The product of *o*-Methoxybenzaldehyde (600 MHz, DMSO-d_6) δ 8.48 (s, 1H), 7.97 (dd, *J* = 7.9, 1.6 Hz, 1H), 7.68 (ddd, *J* = 8.7, 7.3, 1.7 Hz, 1H), 7.24 (dd, *J* = 8.5, 1.0 Hz, 1H), 7.18-7.12 (m, 1H), 3.91 (s, 3H).[30]

The product of *p*-Methoxybenzaldehyde (400 MHz, $CDCl_3$): δ 7.78 (1H, s), 7.52-7.44 (3H, m), 7.23-7.19 (1H, m), 3.19 (3H, s).[31]

The product of *p*-Methoxybenzaldehyde (500 MHz, $CDCl_3$) δ 7.90 (d, *J* = 8.9 Hz, 2H), 7.64 (s, 1H), 7.00 (d, *J* = 9.0 Hz, 2H), 3.91 (s, 3H).[32]

The product of 4-Biphenylcarboxaldehyde (400 MHz, $CDCl_3$) δ 8.01 (d, *J* = 8.4 Hz, 2H, ArH), 7.80 (d, *J* = 3.7 Hz, 2H, ArH), 7.78 (s, 1H, CH), 7.67 (d, *J* = 7.1 Hz, 2H, ArH), 7.52 (t, *J* = 7.3 Hz, 2H, ArH), 7.48 (d, *J* = 7.1 Hz, 1H, ArH).[33]

The product of 4-Benzyloxybenzaldehyde ($CDCl_3$) δ 5.18 s (2H, CH_2), 7.11 d (2H, *J* = 8.7 Hz), 7.38-7.47 m (5H), 7.87 d (2H, *J* = 8.7 Hz), 9.91 s (1H, CHO).[34]

The product of *p*-Chlorobenzaldehyde (500 MHz, DMSO) δ 8.57 (s, 1H), 7.97 (d, *J* = 8.6 Hz, 2H), 7.73 (d, *J* = 8.6 Hz, 2H).[35]

The Method for Calculating the Conversion

Cyanosilylation and Knoevenagel Condensation 1,3,5-Trimethoxybenzene had 3 H protons on benzene ring (δ ppm = 6.10). All the products had 1 H proton on their chiral C atom. Consequently, the yield of the reactions could be read from the ^1H spectrum directly, as the same amount of 1,3,5-trimethoxybenzene (compared to the aldehyde) was added into the system before monitoring the ^1H spectra.

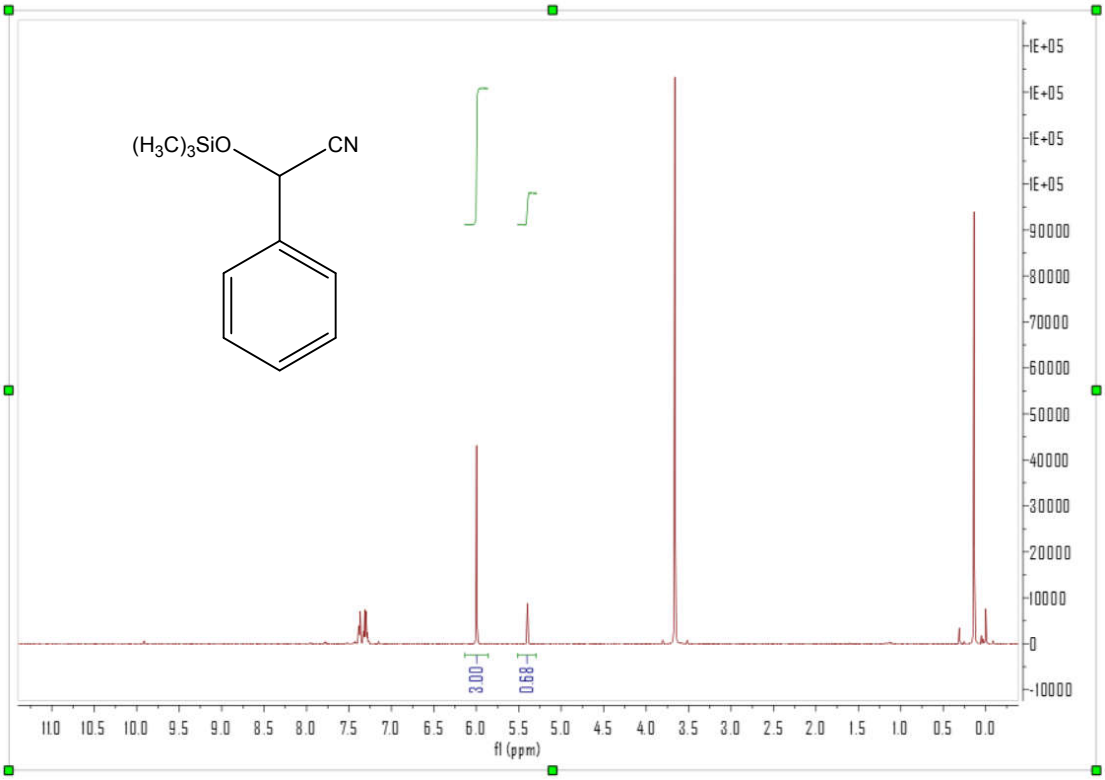

Figure S24. ^{1}H-NMR for cyanosilylation of benzaldehyde (1.2 mmol TMSCN, 0.5 mmol aldehydes, and 0.01 mmol Ce-4L in DCM for 12 h).

Yield = 68%

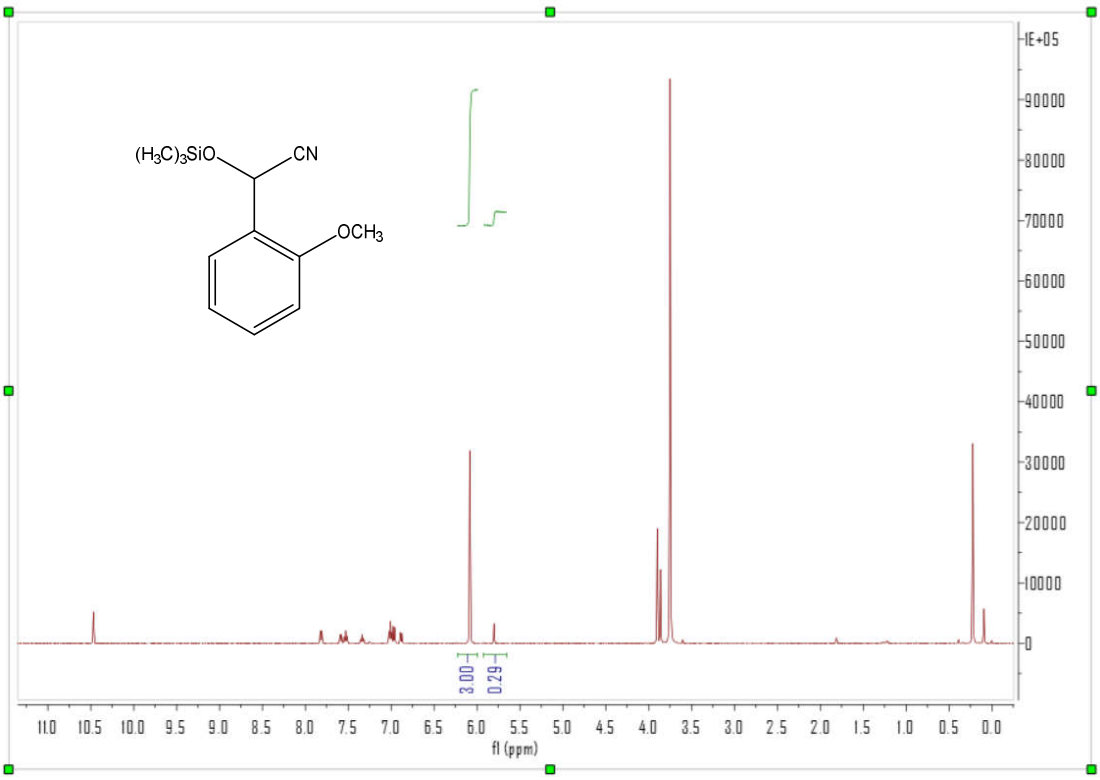

Figure S25. ^{1}H-NMR for cyanosilylation of 2-methoxybenzaldehyde (1.2 mmol TMSCN, 0.5 mmol aldehydes, and 0.01 mmol Ce-4L in DCM for 12 h).

Yield = 29%

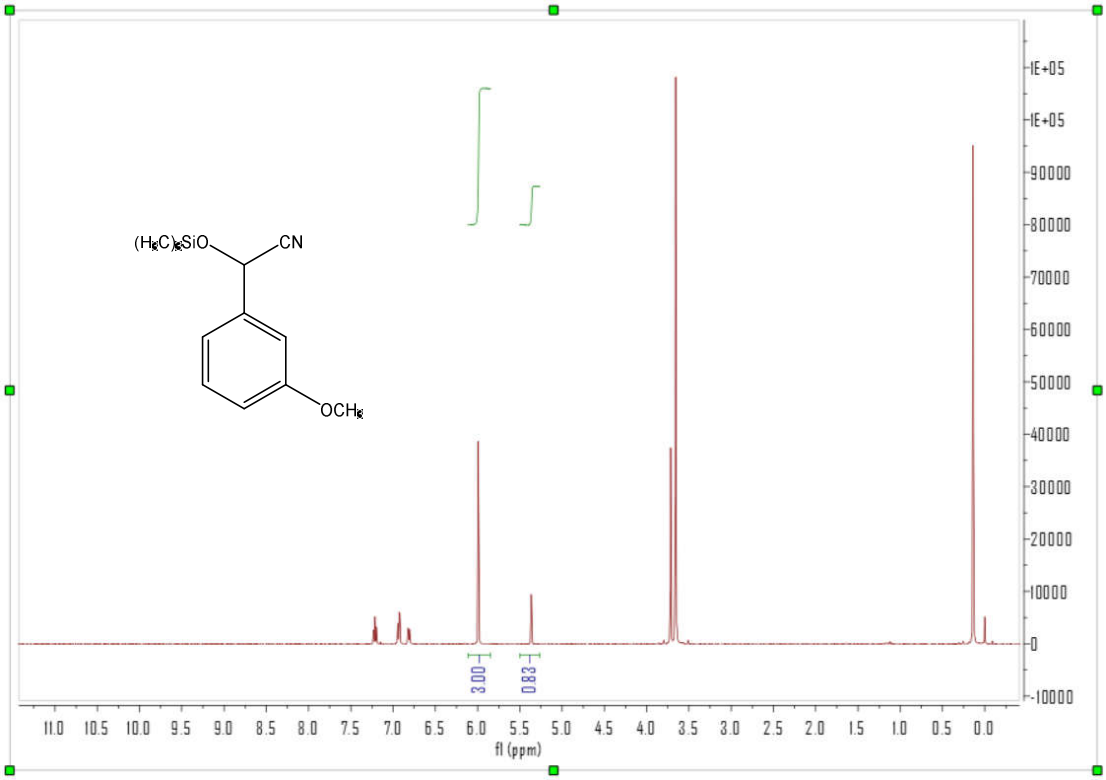

Figure S26. ^{1}H-NMR for cyanosilylation of 3-methoxybenzaldehyde (1.2 mmol TMSCN, 0.5 mmol aldehydes, and 0.01 mmol Ce-4L in DCM for 12 h).

Yield = 83%

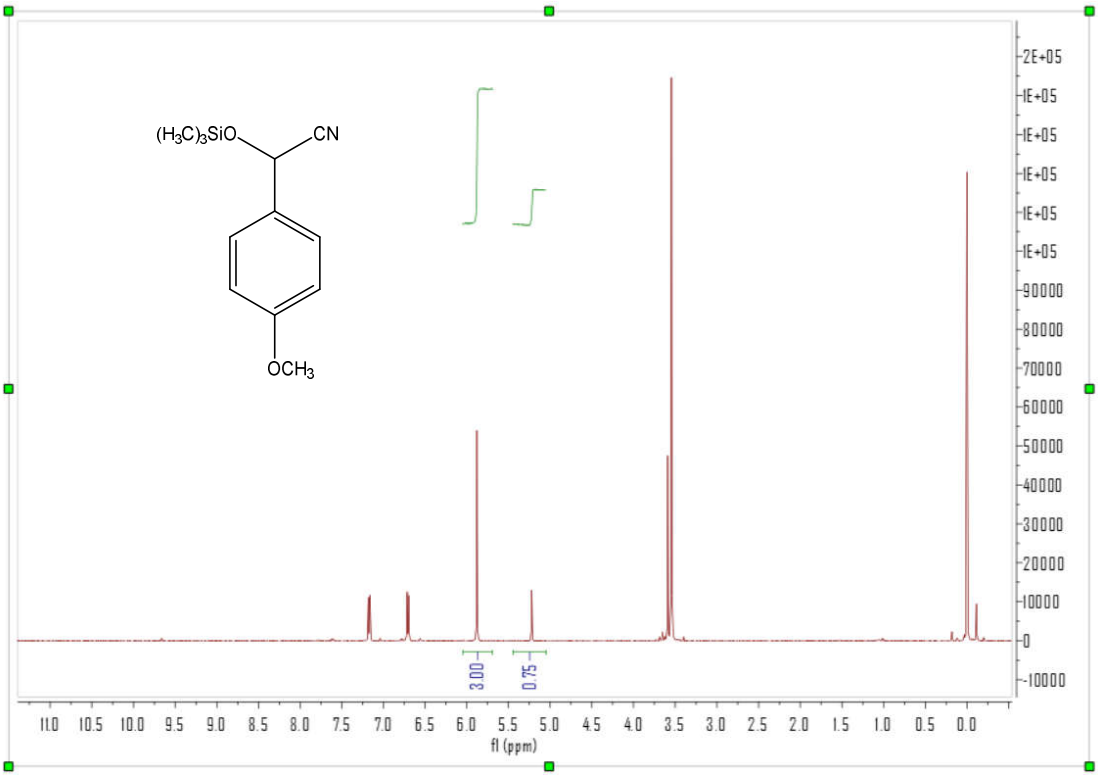

Figure S27. ^{1}H-NMR for cyanosilylation of 4-methoxybenzaldehyde (1.2 mmol TMSCN, 0.5 mmol aldehydes, and 0.01 mmol Ce-4L in DCM for 12 h).

Yield = 75%

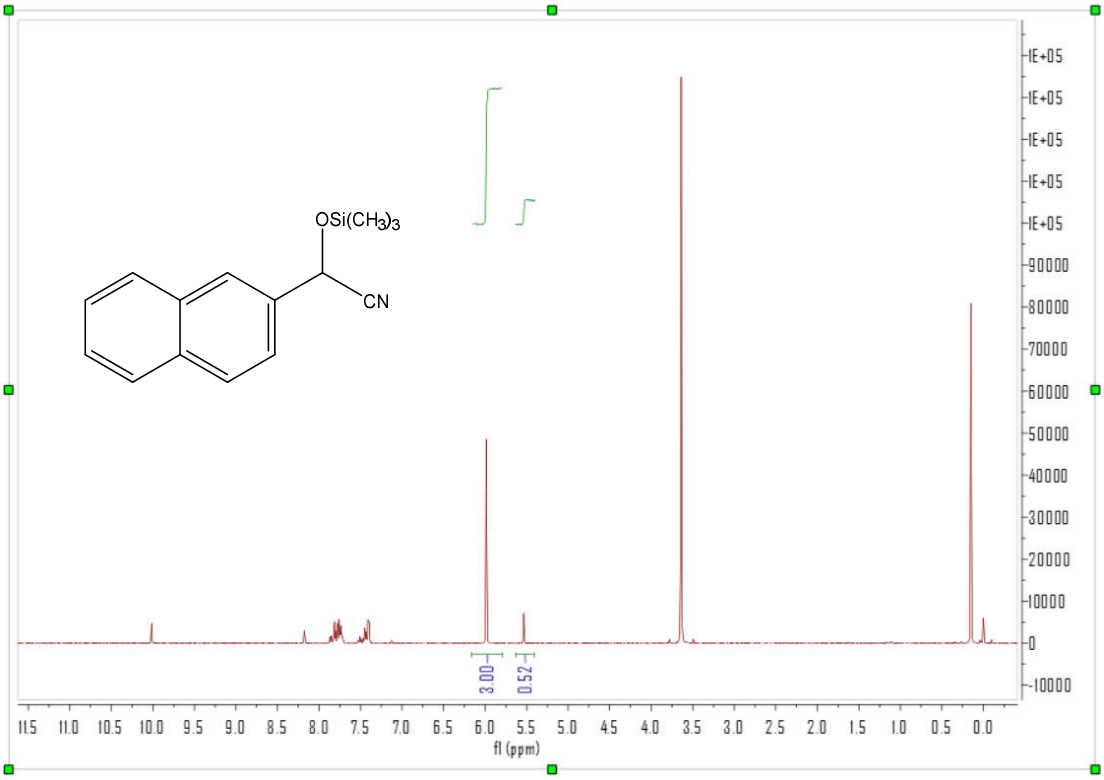

Figure S28. ^{1}H-NMR for cyanosilylation of 2-naphthaldehyde (1.2 mmol TMSCN, 0.5 mmol aldehydes, and 0.01 mmol Ce-4L in DCM for 12 h).

Yield = 52%

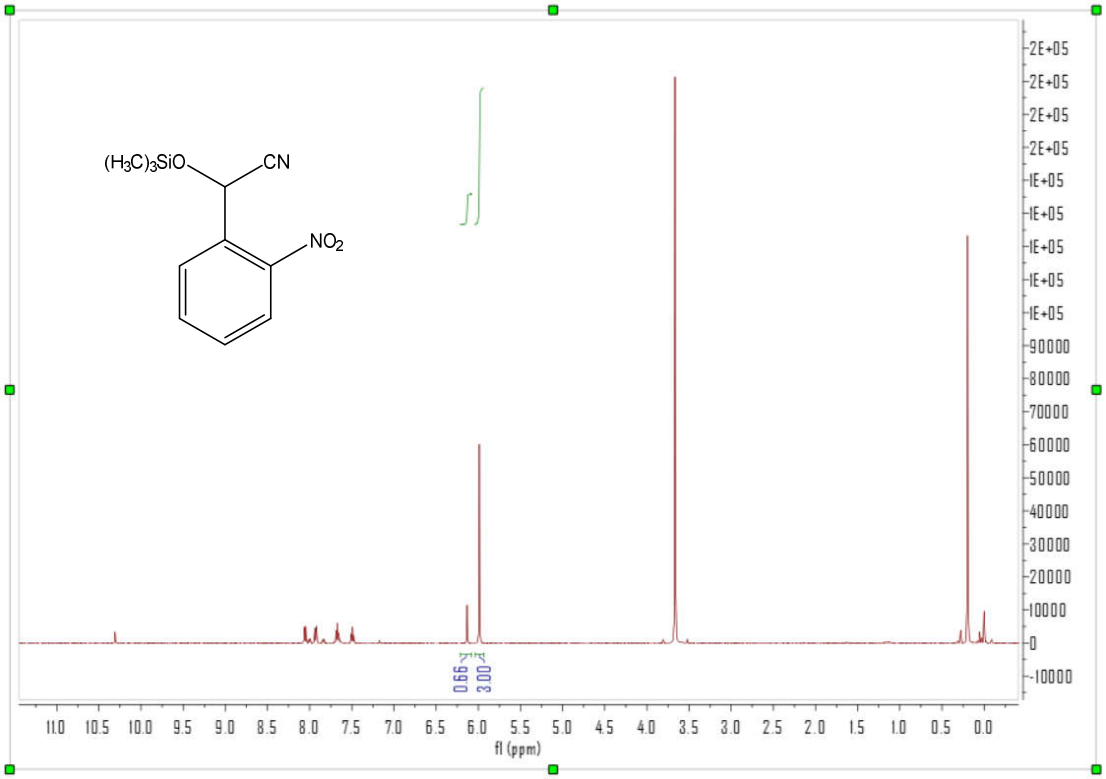

Figure S29. ^{1}H-NMR for cyanosilylation of 2-nitrobenzaldehyde (1.2 mmol TMSCN, 0.5 mmol aldehydes, and 0.01 mmol Ce-4L in DCM for 12 h).

Yield = 66%

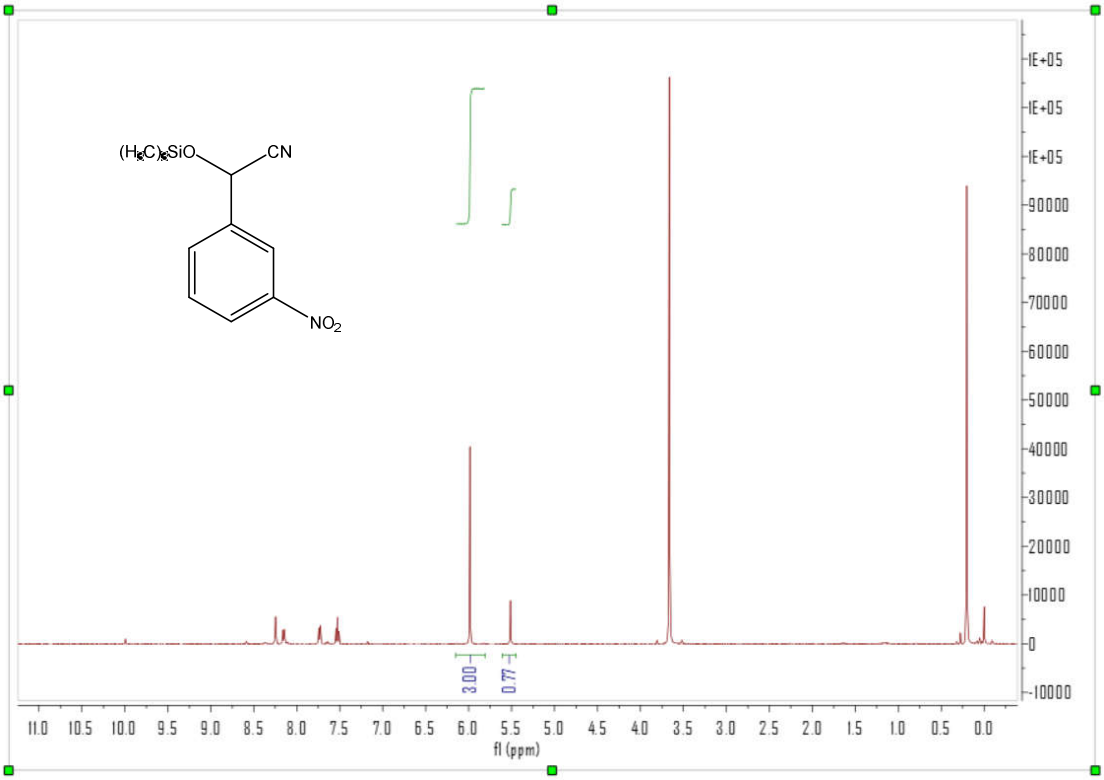

Figure S30. ^{1}H-NMR for cyanosilylation of 3-nitrobenzaldehyde (1.2 mmol TMSCN, 0.5 mmol aldehydes, and 0.01 mmol Ce-4L in DCM for 12 h).

Yield = 77%

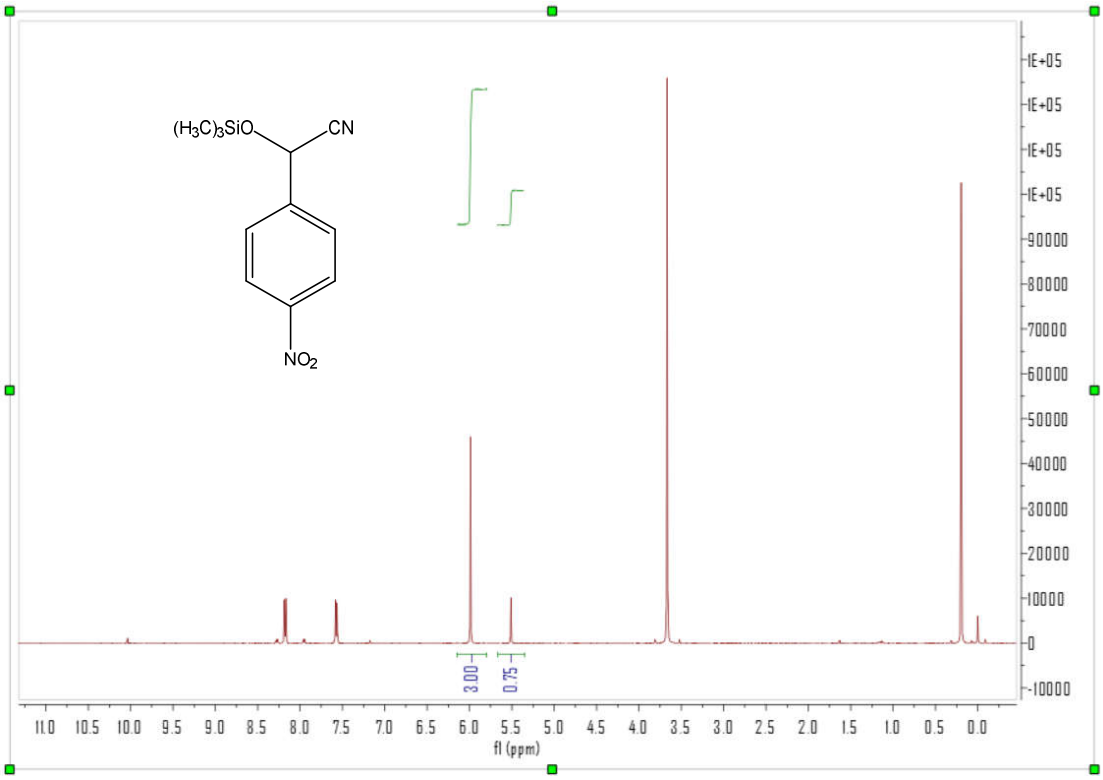

Figure S31. ^{1}H-NMR for cyanosilylation of 4-nitrobenzaldehyde (1.2 mmol TMSCN, 0.5 mmol aldehydes, and 0.01 mmol Ce-4L in DCM for 12 h).

Yield = 75%

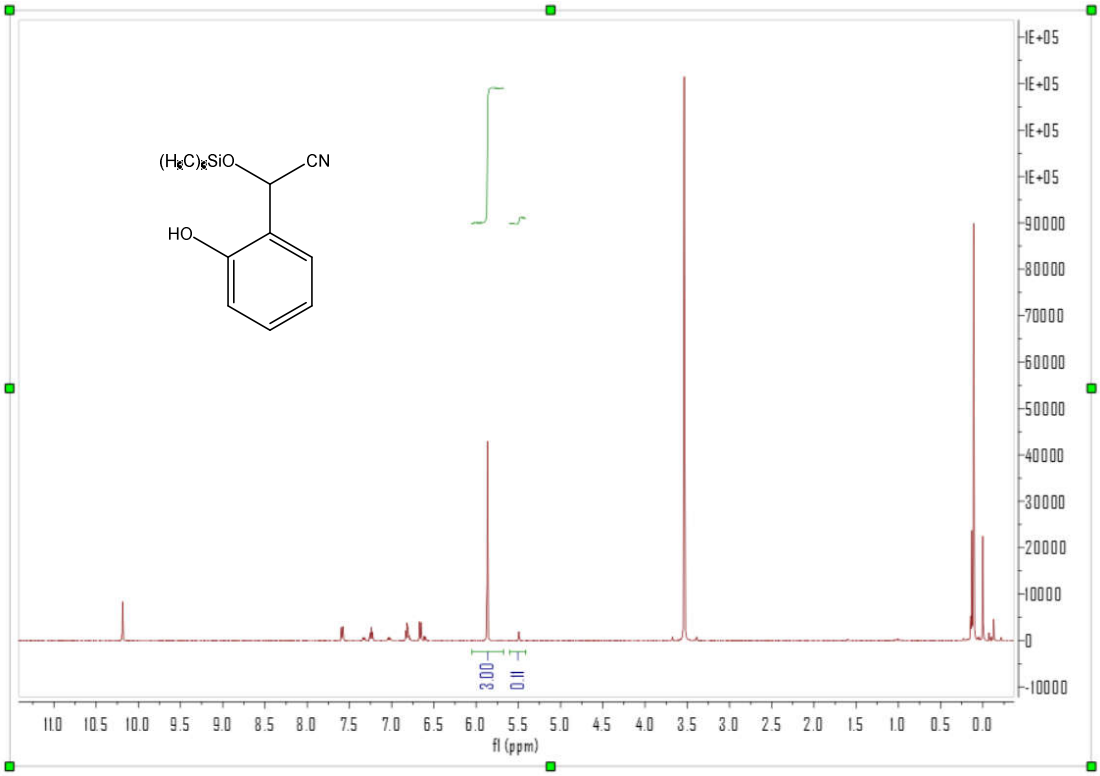

Figure S32. ^{1}H-NMR for cyanosilylation of salicylaldehyde (1.2 mmol TMSCN, 0.5 mmol aldehydes, and 0.01 mmol Ce-4L in DCM for 12 h).

Yield = 11%

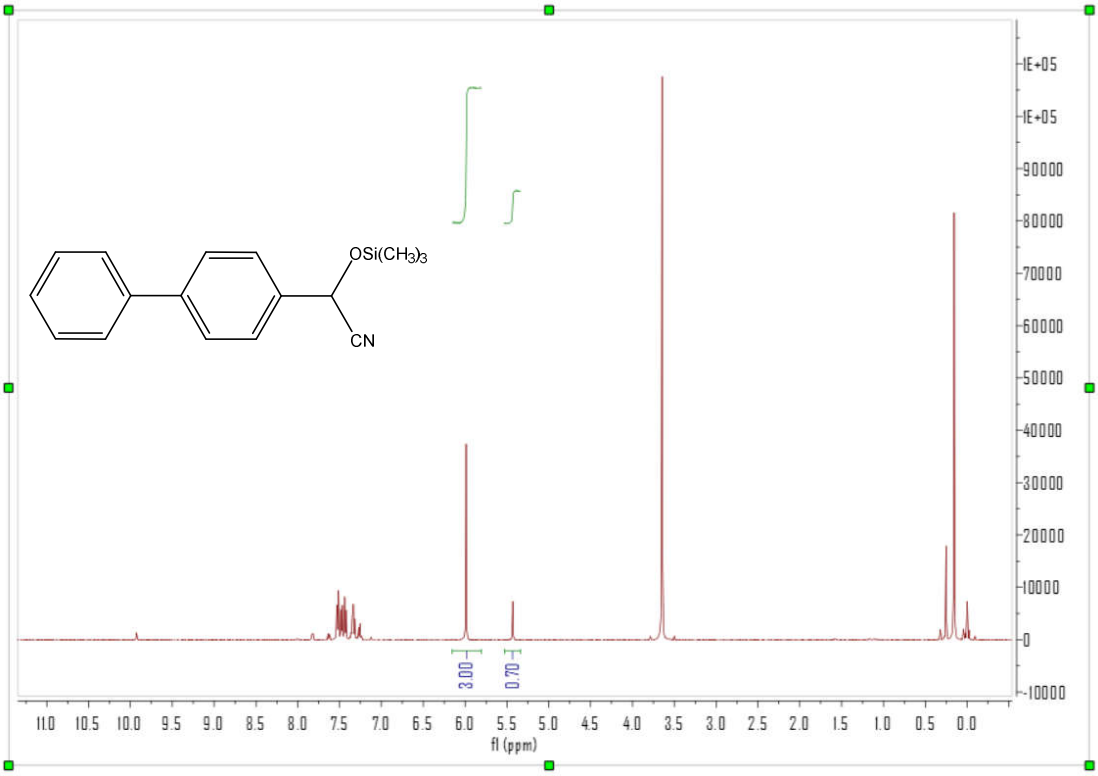

Figure S33. ^{1}H-NMR for cyanosilylation of 4-biphenylcarboxaldehyde (1.2 mmol TMSCN, 0.5 mmol aldehydes, and 0.01 mmol Ce-4L in DCM for 12 h).

Yield = 70%

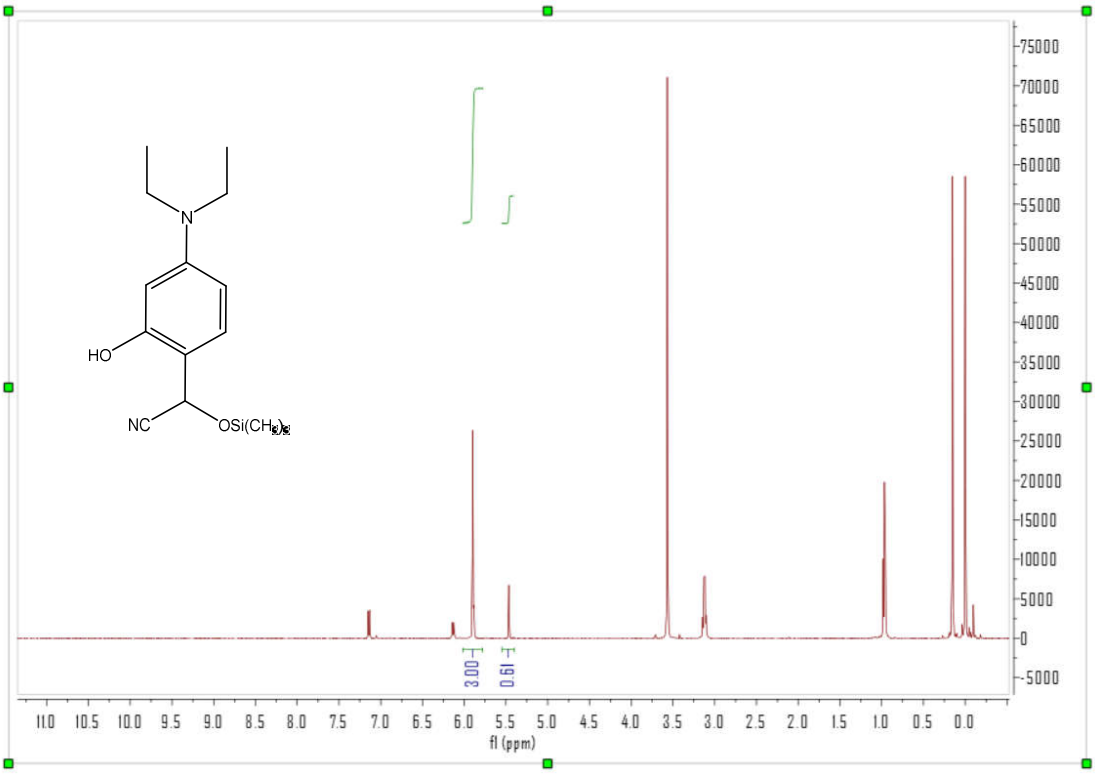

Figure S34. ^{1}H-NMR for cyanosilylation of 4-(diethylamino)salicylaldehyde (1.2 mmol TMSCN, 0.5 mmol aldehydes, and 0.01 mmol Ce-4L in DCM for 12 h).

Yield = 61%

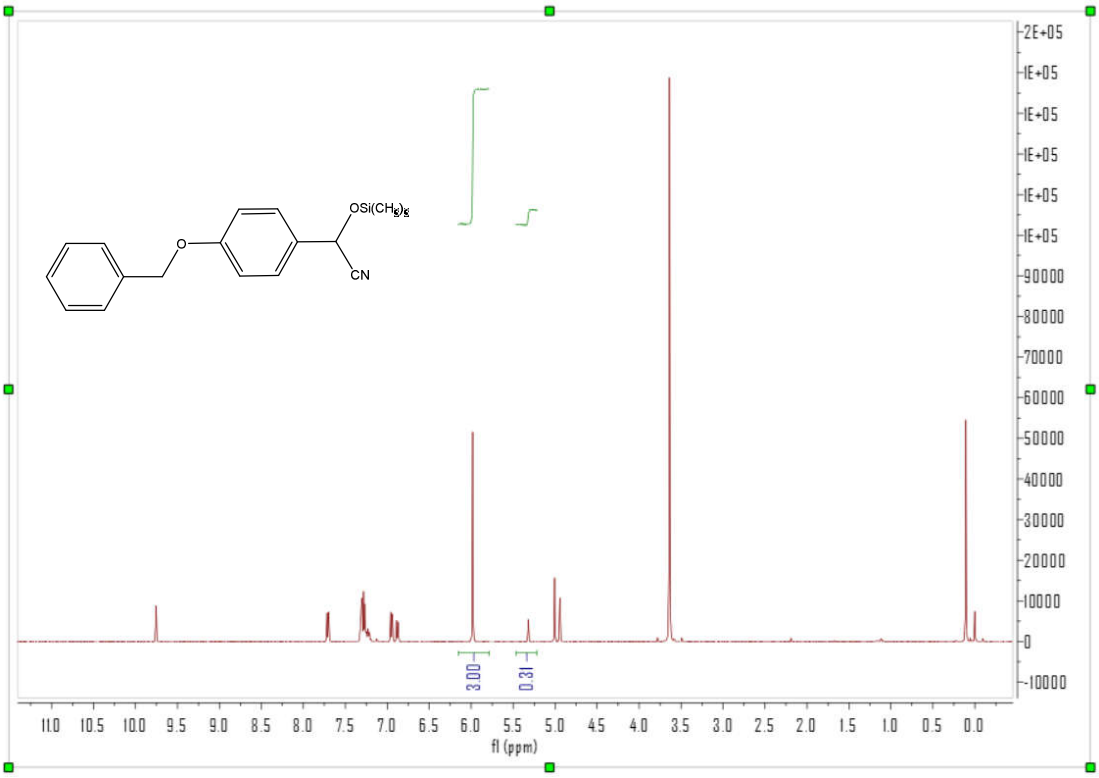

Figure S35. ^{1}H-NMR for cyanosilylation of 4-benzyloxybenzaldehyde (1.2 mmol TMSCN, 0.5 mmol aldehydes, and 0.01 mmol Ce-4L in DCM for 12 h).

Yield = 31%

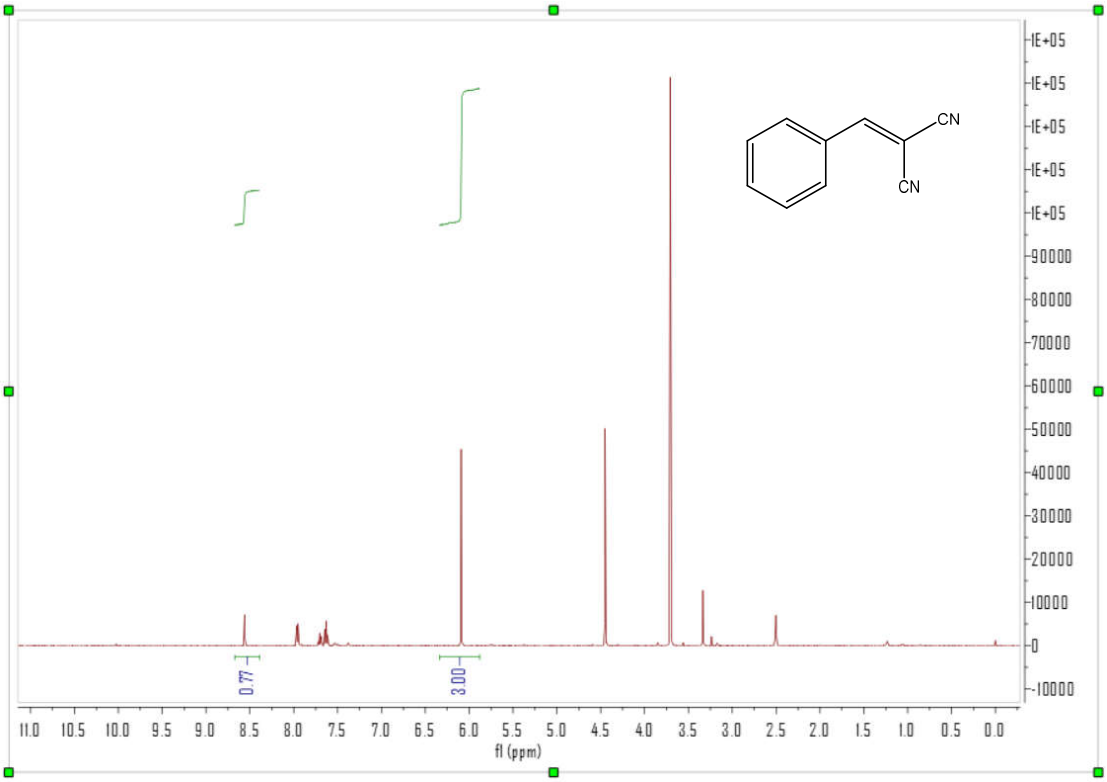

Figure S36. ^{1}H-NMR for Knoevenagel condensation of benzaldehyde (1.2 mmol malononitrile, 0.5 mmol aldehydes, and 0.01 mmol Ce-4L in chloroform for 12 h).

Yield = 77%

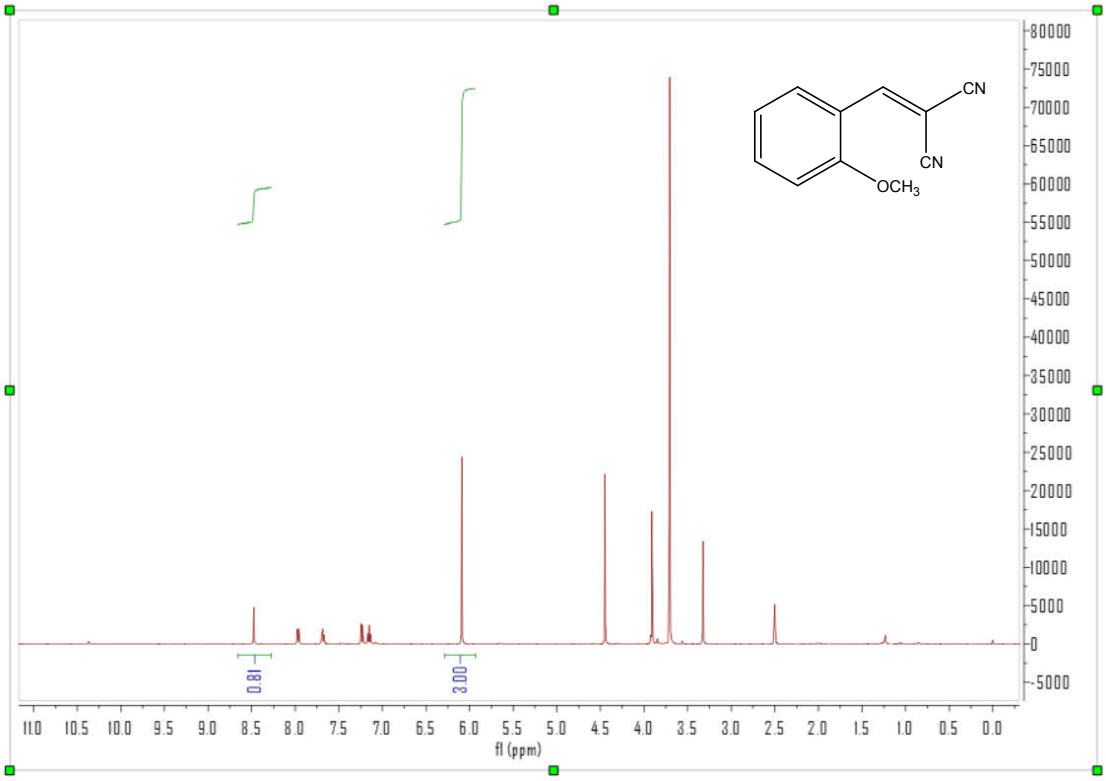

Figure S37. ^{1}H-NMR for Knoevenagel condensation of 2-methoxybenzaldehyde (1.2 mmol malononitrile, 0.5 mmol aldehydes, and 0.01 mmol Ce-4L in chloroform for 12 h).

Yield = 81%

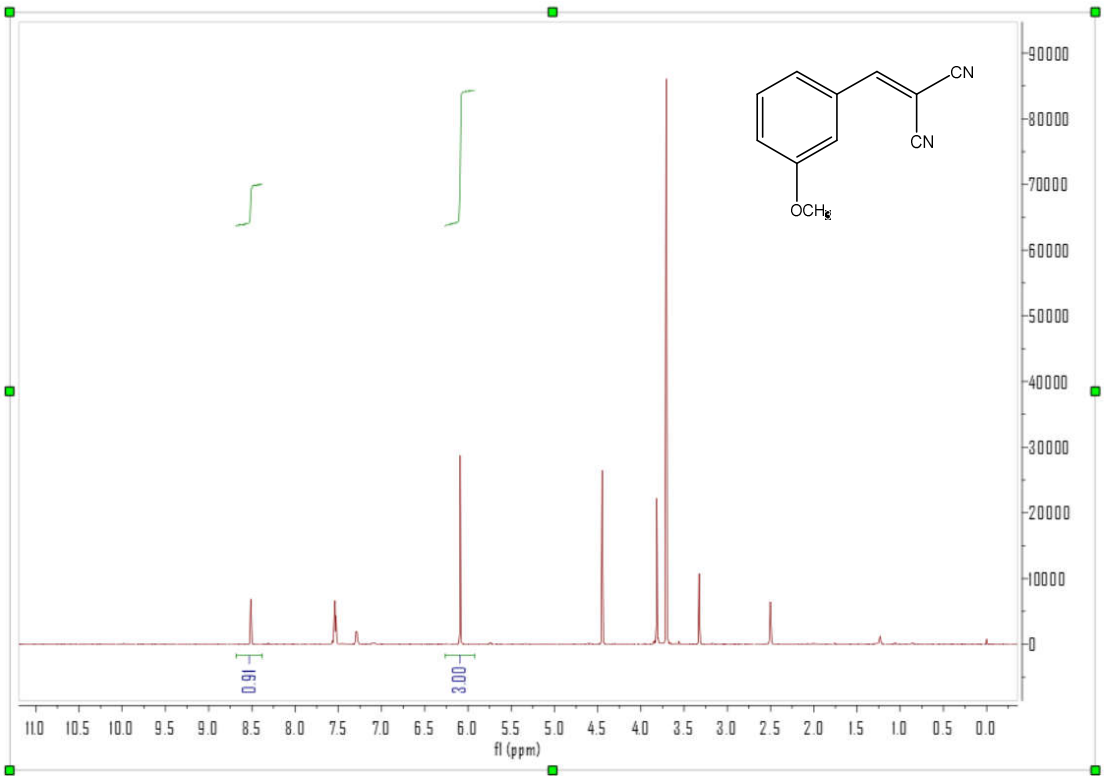

Figure S38. ^{1}H-NMR for Knoevenagel condensation of 3-methoxybenzaldehyde (1.2 mmol malononitrile, 0.5 mmol aldehydes, and 0.01 mmol Ce-4L in chloroform for 12 h).

Yield = 91%

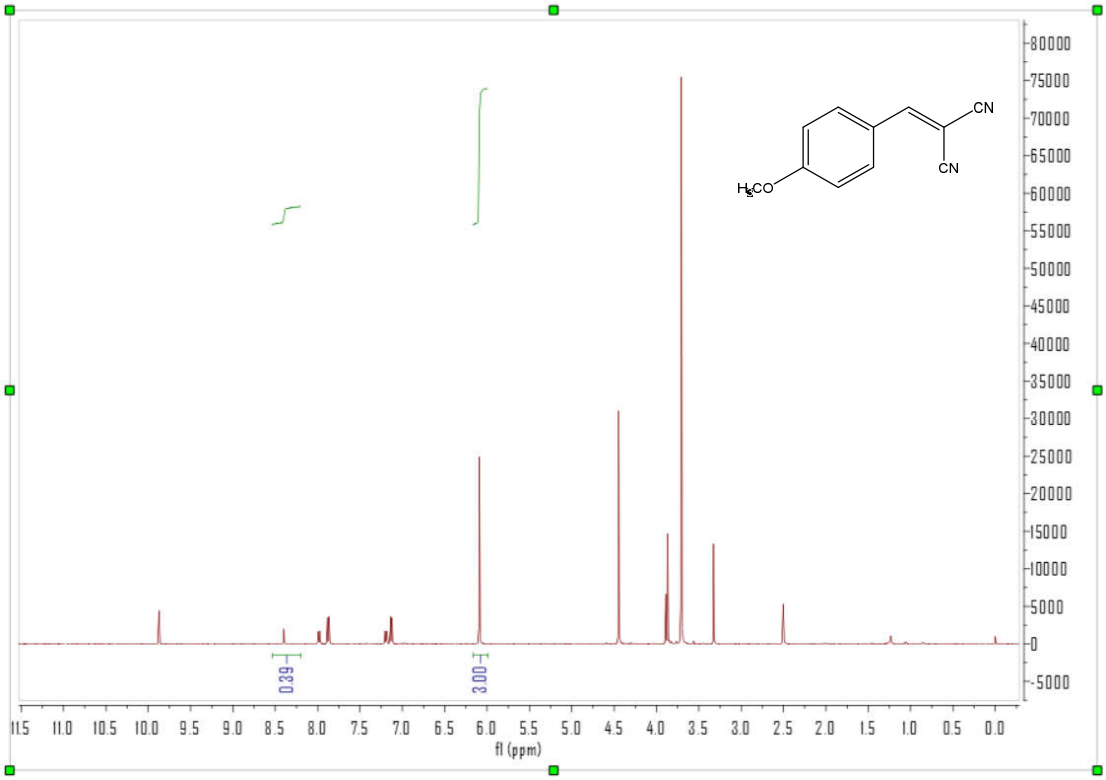

Figure S39. ^{1}H-NMR for Knoevenagel condensation of 4-methoxybenzaldehyde (1.2 mmol malononitrile, 0.5 mmol aldehydes, and 0.01 mmol Ce-4L in chloroform for 12 h).

Yield = 39%

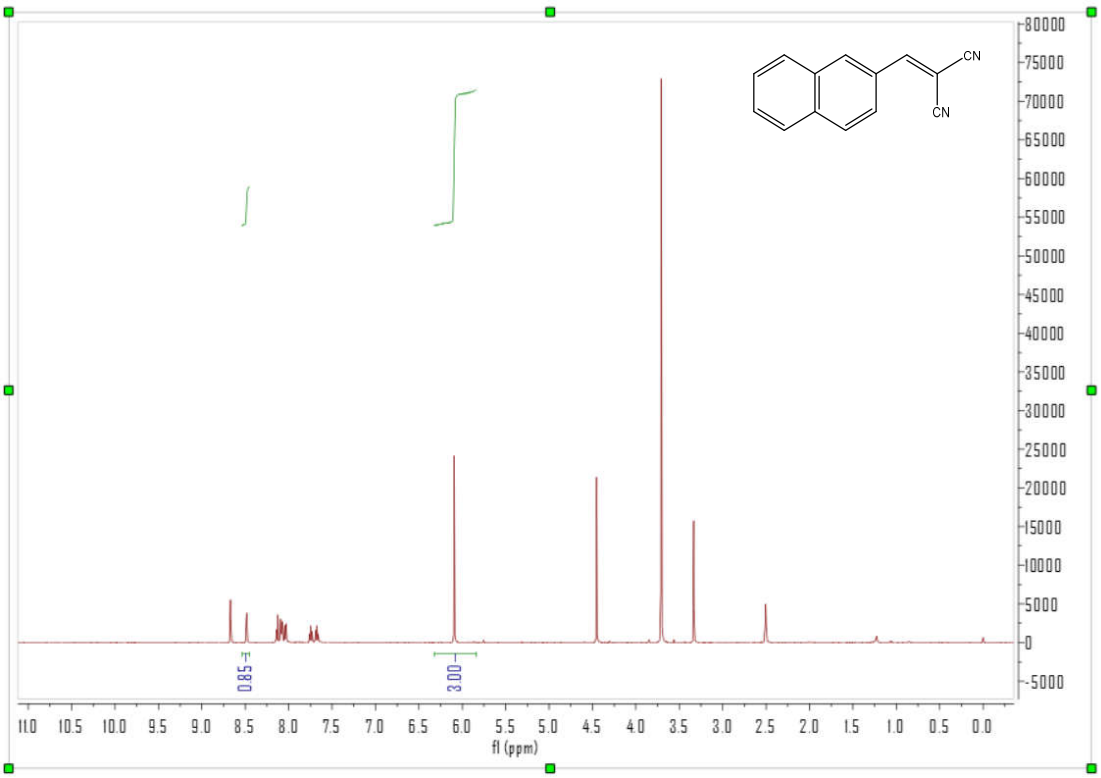

Figure S40. ^{1}H-NMR for Knoevenagel condensation of 2-naphthaldehyde (1.2 mmol malononitrile, 0.5 mmol aldehydes, and 0.01 mmol Ce-4L in chloroform for 12 h).

Yield = 85%

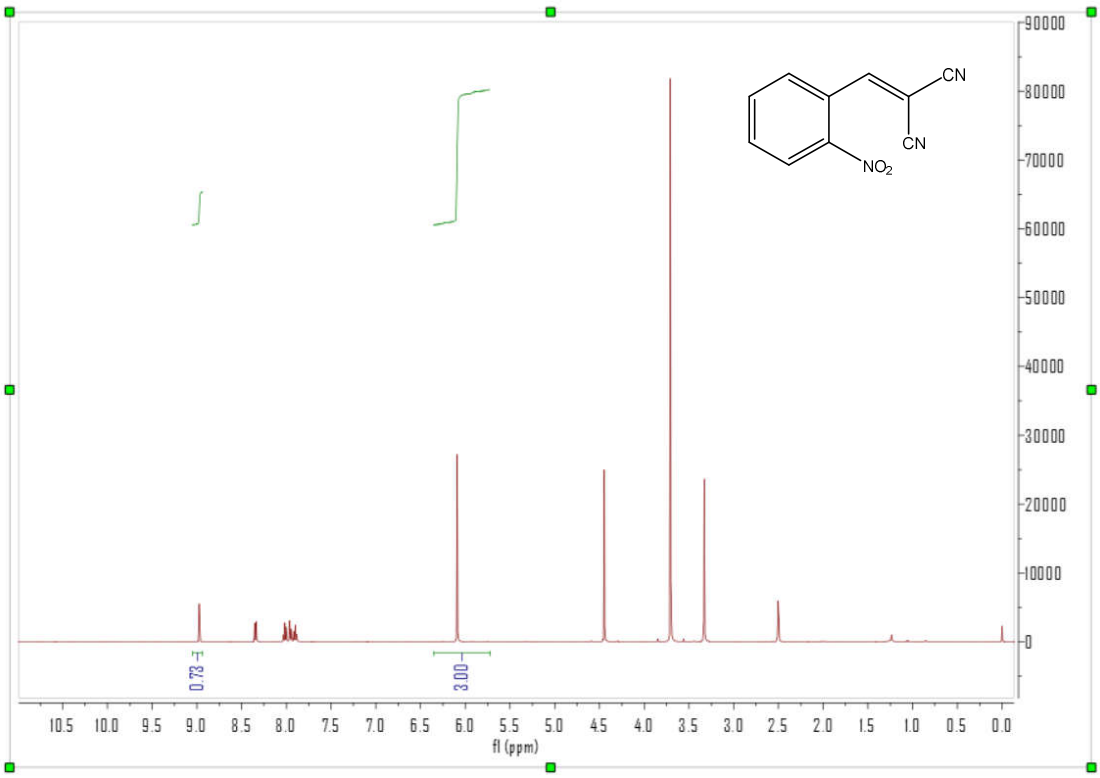

Figure S41. ^{1}H-NMR for Knoevenagel condensation of 2-nitrobenzaldehyde (1.2 mmol malononitrile, 0.5 mmol aldehydes, and 0.01 mmol Ce-4L in chloroform for 12 h).

Yield = 73%

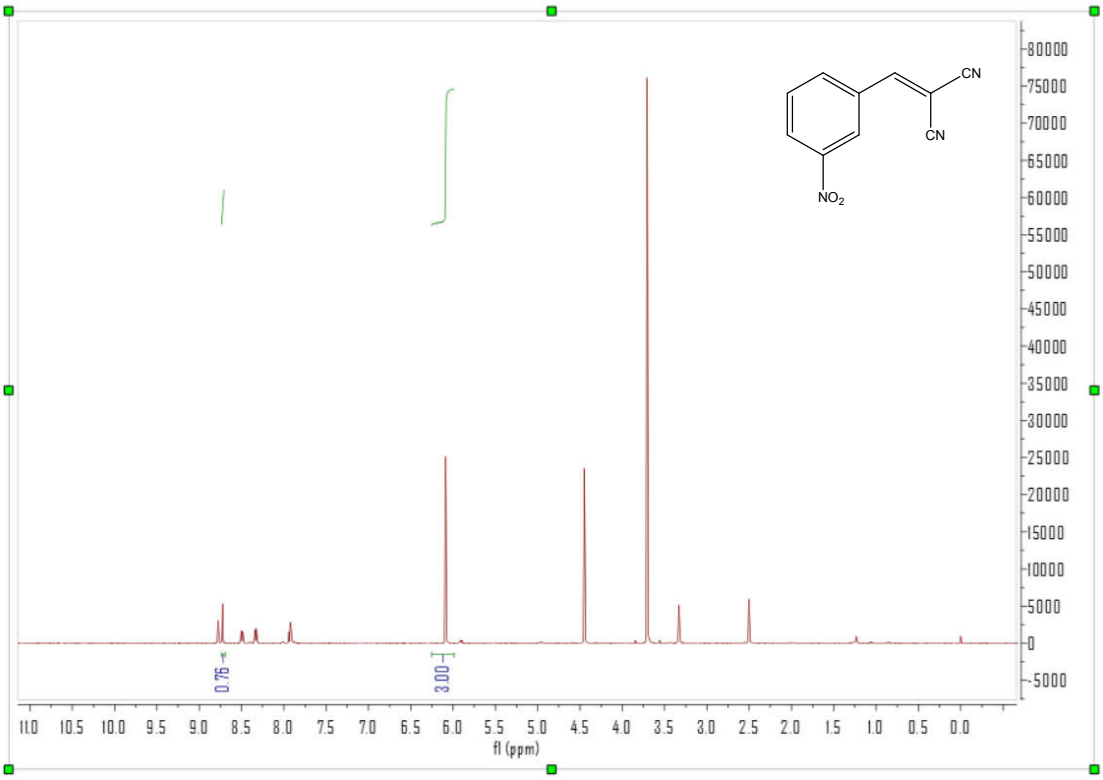

Figure S42. ^{1}H-NMR for Knoevenagel condensation of 3-nitrobenzaldehyde (1.2 mmol malononitrile, 0.5 mmol aldehydes, and 0.01 mmol Ce-4L in chloroform for 12 h).

Yield = 76%

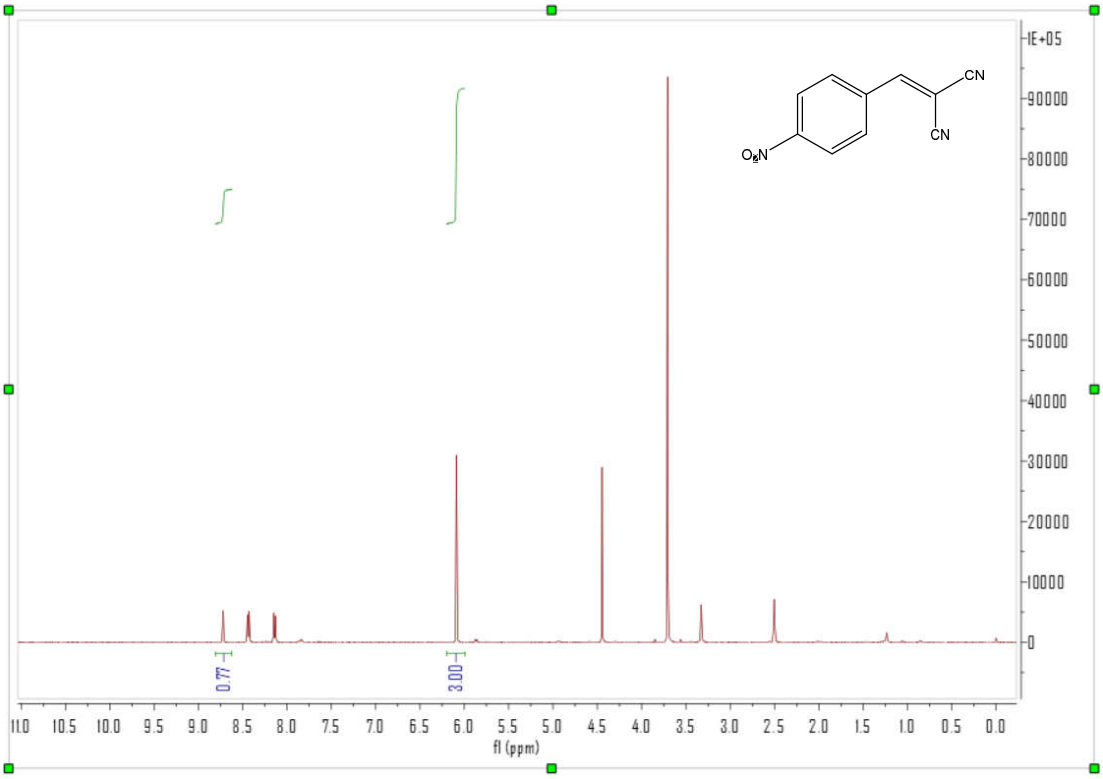

Figure S43. ^{1}H-NMR for Knoevenagel condensation of 4-nitrobenzaldehyde (1.2 mmol malononitrile, 0.5 mmol aldehydes, and 0.01 mmol Ce-4L in chloroform for 12 h).

Yield = 77%

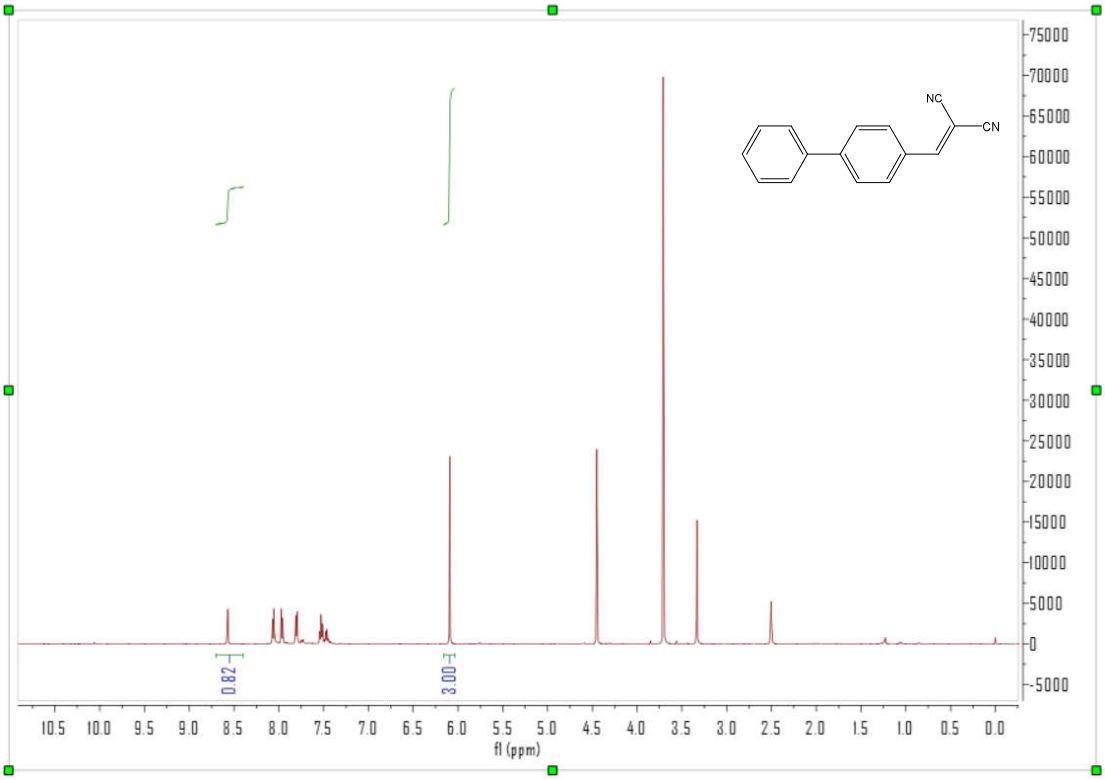

Figure S44. ^{1}H-NMR for Knoevenagel condensation of 4-biphenylcarboxaldehyde (1.2 mmol malononitrile, 0.5 mmol aldehydes, and 0.01 mmol Ce-4L in chloroform for 12 h).

Yield = 82%

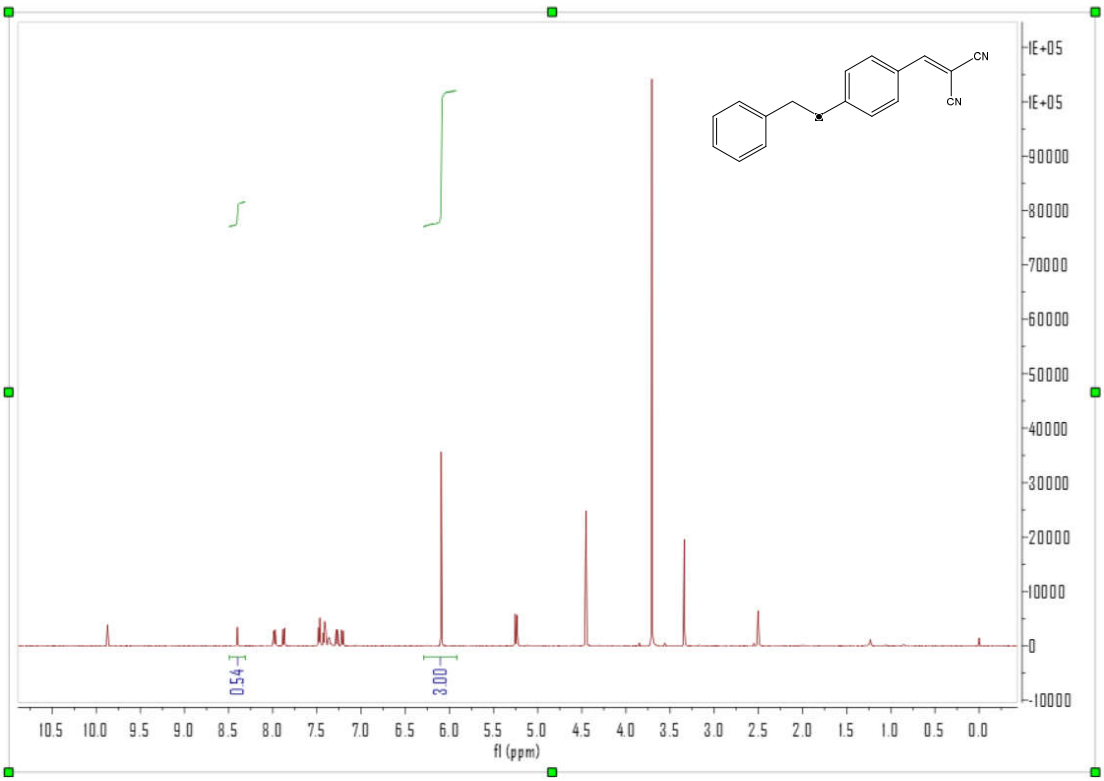

Figure S45. ^{1}H-NMR for Knoevenagel condensation of 4-benzyloxybenzaldehyde (1.2 mmol malononitrile, 0.5 mmol aldehydes, and 0.01 mmol Ce-4L in chloroform for 12 h).

Yield = 54%

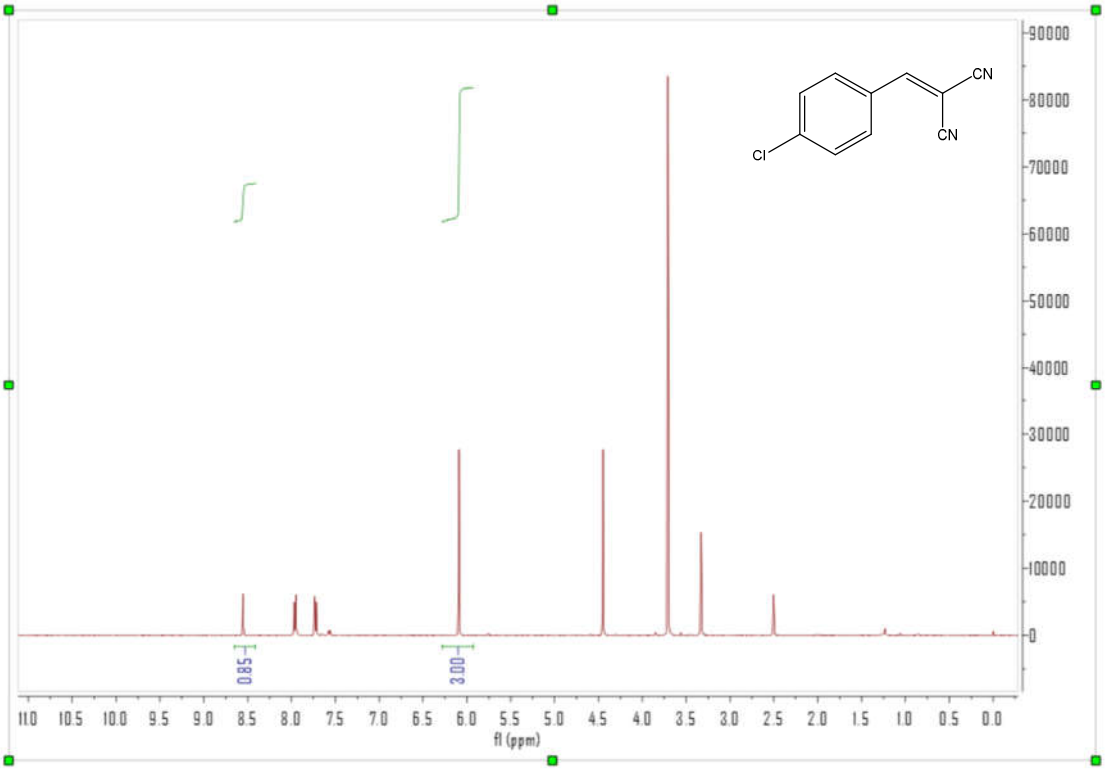

Figure S46. ^{1}H-NMR for Knoevenagel condensation of *p*-chlorobenzaldehyde (1.2 mmol malononitrile, 0.5 mmol aldehydes, and 0.01 mmol Ce-4L in chloroform for 12 h).

Yield = 85%

References

(1) L. K. Meng, K. Liu, S. Fu, L. Wang, C. Liang, G. H. Li, C. G. Li and Z. Shi, *Journal of Solid State Chemistry*, 2018, 265, 285-290.
(2) T. J. Sum, T. H. Sum, W. R. Galloway, D. G. Twigg, J. J. Ciardiello and D. R. Spring, *Tetrahedron*, 2018, 74, 5089-5101.
(3) B. Hasanpour, M. Jafarpour, A. Eskandari and A. Rezaeifard, *Eur. J. Org. Chem*., 2020, 4122-4129.
(4) B. Hong, K. C. C. Aganda and A. Lee, *Org. Lett.*, 2020, 22, 4395-4399.
(5) B. Zhao, R. Shang, W. M. Cheng and Y. Fu, *Org. Chem. Front.*, 2018, 5, 1782-1786.
(6) S. Kim, J. Lee, S. Jeoung, H. R. Moon and M. Kim, *Chem. Eur. J.*, 2020, 26, 7568-7572.
(7) I. Ibrahem, M. N. Iqbal, O. Verho, A. Eivazihollagh, P. Olsen, H. Edlund, C. W. Tai, M. Norgren and E. V. Johnston, *ChemNanoMat*, 2018, 4, 71-75.
(8) W. Zhang, Z. Q. Xiao, J. J. Wang, W. Q. Fu, R. Tan and D. H. Yin, *ChemCatChem* 2019, 11, 1779-1788.
(9) M. Ali, T. Reza and G. Reza, *Combinatorial Chemistry & High Throughput Screening*, 2020*,* 23, 119-125.
(10) Y. J. Mao, Y. Liu, Y. W. Hu, L. Wang, S. L. Zhang and W. Wang, *ACS Catal.*, 2018, 8, 3016-3020.
(11) S. T. Hulushe, M. H. Manyeruke, M. Louzada, S. Rigin, E. C. Hosten and G. M. Watkins, *RSC Adv.*, 2020, 10, 16861-16874.
(12) D. E. Wise, E. S. Gogarnoiu, A. D. Duke, J. M. Paolillo, T. L. Vacala, W. A. Hussain and M. Parasram, *J. Am. Chem. Soc.*, 2022, 144, 15437-15442.
(13) E. Sheikhi, M. Adib, M. A. Karajabad and N. Rezaei, *ChemistrySelect*, 2019, 4, 13455-13458.
(14) B. Karimi and L. Ma'mani, *Org. Lett.*, 2004, 6, 4813-4815.
(15) M. K. Sharma, S. Sinhababu, G. Mukherjee, G. Rajaraman and S. Nagendran, *Dalton Trans*., 2017, 46, 7672-7676.
(16) J. Li, T. Yu, M. Luo, Q. Xiao, W. W. Yao, L. Xu and M. T. Ma, *Journal of Organometallic Chemistry*, 2018, 874, 83-86.
(17) S. Yadav, R. Dixit, K. Vanka and S. S. Sen, *Chem. Eur. J.*, 2018, 24, 1269-1273.
(18) J. Krieger, T. Smeilus, O. Schackow and A. Giannis, *Chem. Eur. J.*, 2017, 23, 5000-5004.
(19) Z. G. Zhang, J. W. Chen, Z. B. Bao, G. G. Chang, H. B. Xing and Q. L. Ren, *RSC Adv*., 2015, 5, 79355-79360.
(20) J. S. Kramer, S. Woltersdorf, T. Duflot, K. Hiesinger, F. F. Lilich, F. Knoll, S. K. Wittmann, F. M. Klingler, S. Brunst, A. Chaikuad, C. Morisseau,; B. D. Hammock,; C. Buccellati, A. Sala, G. E. Rovati, M.Leuillier, S. Fraineau, J. Rondeaux, V. Hernandez-Olmos, J. Heering, D. Merk, D. Pogoryelov, D. Steinhilber, S. Knapp, J. Bellien and E. Proschak, *J. Med. Chem.*, 2019, 62, 8443-8460.
(21) A. Karmakar, Rubio, M. D. M. R. Guilherme, A. Paul, M. F. C. G. Silva, T. K. Mahmudov, F. I. Guseinov, S. A. C. Carabineiro and A. J. L. Pombeiro, *Dalton Trans*., 2017, 46, 8649-8657.
(22) H. Yang, Y. L. Shen, Z. H. Xiao, C. Y. Liu, K. D. Yuan and Y. Ding, *Chem. Commun.*, 2020, 56, 2435-2438.
(23) Z. Chen, J. Wang, Y. N. Zhu and M. Q. Ge, *Dyes and Pigments*, 2017, 143, 190-195.
(24) G. Rajagopal, S. S. Kim and S. C. George, *Appl. Organometal. Chem.*, 2007, 21, 198-202.
(25) J. M. Perez, S. Rojas, A. Garcia-Garcia, H. Montes-Andres, C. R. Martinez, M. S. Romero-Cano, D. Choquesillo-Lazarte,; V. K. Abdelkader-Fernandez, M. Perez-Moendoza, J. Cepeda, A. Rodriguez-Dieguez and I. Fernandez, *Inorg. Chem.*, 2022, 61, 1377-1384.
(26) P. A. Burate, R. J. Balasaheb, P. H. Desale and A. K. Kinage, *Catalysis Letters*, 2019, 149, 2368-2375.
(27) R. Takakura, K. Koyama, M. Kuwata, T. Yamada, H. Sajiki and Y. Sawama, *Organic & Biomolecular Chemistry*, 2020, 18, 6594-6597.
(28) A. Das, N. Anbu, M. SK, A. Dhakshinamoorthy and S. Biswas, *European Journal of Inorganic Chemistry*, 2020, 29, 2830-2834.
(29) H. X. Lv, L. M. Fan, H. T. Chen, X. T. Zhang and Y. P. Gao, *Dalton Transactions*, 2022, 51, 3546-3556.
(30) W. G. Zuo, S. B. Yang, Y. J. Xing, X. W. Xiao, D. N. Fan, H. Y. Li, G. Q. Wang, B. Qin,; S. You and X.Jia, *Dalton Transactions*, 2022, 51, 6631-6637.
(31) M. Tavakolian and M. M. Najafpour, *New Journal of Chemistry*, 2019, 43, 16437-16440.
(32) W. J. Ang, Y. S. Chng and Y. L. Lam, *RSC Adv.*, 2015, 5, 81415-81428.

(33) K. Gong, D. Q. Zhang, Y. Y. Wang, C. H. Li, H. M. Zhang, H. R. Li and H. R. Feng, *Molecular Catalysis* ,2021, 509, 111663.
(34) S. A. Lermontova, I. S. Grigor'ev, N. N. Peskova,; E. Yu. Ladilina, I. V. Balalaeva, L. G. Klapshina and V. P. Boyarskii, *Russian Journal of General Chemistry*, 2017, 87, 479-484.
(35) Z. T. Wang, X. F. Yuan, Q. A. Cheng, T. C. Zhang and J. Luo, *New Journal of Chemistry*, 2018, 42, 11610-11615.